Combined phylogenetic analysis of two new Afrotropical genera of Onthophagini (Coleoptera, Scarabaeidae)

Combined phylogenetic analysis of two new Afrotropical genera of Onthophagini (Coleoptera, Scarabaeidae)

ANGELA ROGGERO[1]*, MICHAEL DIERKENS[2], ENRICO BARBERO[1], CLAUDIA PALESTRINI[1]

[1]Department of Life Sciences and Systems Biology, Via Accademia Albertina 13 – I-10123 Torino, ITALY

[2]rue du Garet 21, F – 69001, Lyon, FRANCE

*Corresponding author e-mail: angela.roggero@unito.it

Running title: Phylogeny of Afrotropical Onthophagini

ABSTRACT

To reveal the relationships of the Afrotropical *Onthophagus* 32nd group, a combined phylogenetic analysis was employed on a matrix of both discrete and continuous morphological characters. The species of the 32nd group do not constitute a homogeneous group, but two distinct and well-isolated clades of generic rank: *Hamonthophagus* **gen. nov**. with five species and *Morettius* **gen. nov**. with two species, one of which was identified as a new taxon and is described here (i.e., *Morettius utete* **sp. nov.**). The *Hamonthophagus* species were characterized by a wide distribution covering the entire geographic range of Afrotropical grasslands, while the *Morettius* species were restricted to two distinct areas in central Africa and east Africa. Geographical data were integrated with the phylogenetic results and processed by dispersal-vicariance analysis, which confirmed for both genera an evolutionary and biogeographic history in which the ancestral range was located in the central eastern African region.

ADDITIONAL KEYWORDS: Biogeography, dung beetles, *Hamonthophagus*, *Morettius*, new species, geometric morphometrics, Scarabaeoidea, systematics

INTRODUCTION

In 1913, d'Orbigny proposed a full synopsis of the Afrotropical Onthophagini on the basis of external features, providing a useful identification tool for this megadiverse tribe. Although his work still remains a milestone in the study of Onthophagini, the French author classification has now been challenged by new methods of systematic and phylogenetic investigation. In the meantime many new species have been described from the Afrotropical region. In particular, the most speciose *Onthophagus* genus has been found to exceed 1,000 species (Tarasov & Solodovnikov, 2011), to which the former subdivision into 32 groups by d'Orbigny (1913) does not always apply. The d'Orbigny's classification has been substantially confirmed in a few instances (such as for the genus *Phalops* Erichson, 1848, Barbero *et al.*, 2003), but in other cases it has been profoundly modified (Moretto, 2009; Tagliaferri *et al.*, 2012), highlighting how the majority of *Onthophagus* species groups may, indeed, not be phylogenetically homogeneous. In this regard, it was recently showed that the present taxonomic position of some species (including part of the 32nd group species) is doubtful, being they less close to the other *Onthophagus* than it is usually considered (Roggero *et al.*, 2016). The 32nd species group was thus here examined to evaluate if the hypothesized separation from *Onthophagus* should be confirmed. The group includes only six Afrotropical coprophagous and often nocturnal species, generally characterized by a wide distribution in open environments such as savannah, grasslands and pastures: *Onthophagus acutus* d'Orbigny, 1908, *O. bituberculatus* (Olivier, 1789), *O. depressus* Harold, 1871, *O. fallax* d'Orbigny, 1913, *O. laceratus* Gerstaecker, 1871, and *O. pallens* d'Orbigny, 1908. Some of these species were accidentally introduced at the beginning of the 20th century into North America and Australia (*O. depressus*), and the Antilles (*O. bituberculatus*), where ostensibly they have adapted quite well, without causing problems to the native fauna.

Recently, Wirta *et al.* (2008) included *O. depressus* in their phylogenetic analysis of the Malagasy dung beetle fauna, since this species has also been introduced into Madagascar, hypothesizing a close relationship with the endemic *Mimonthophagus hinnulus* (Klug, 1832), which is nevertheless markedly different in external and internal morphology, and thus might not be so closely related to *O. depressus*.

The species of the 32nd group lack any complex morphological structures on the head or pronotum, unlike the majority of Onthophagini, in which evident exoskeletal structures are relatively common (Emlen *et al.*, 2005, 2006; Moczek, 2006). All of the 32nd group species are ostensibly characterized by low sexual dimorphism, which mainly affects the fore tibiae and the pygidium. Also, these species share similar patterns of intraspecific colour variation, ranging from an evenly black to yellow background with more or less extensive black spots.

Despite their wide distribution, and a certain degree of individual variability, the taxonomic history of these species is less problematic than that of other *Onthophagus* groups. Only few synonymies are recognized and employed, and even fewer subspecies or varieties have been defined (see the Taxonomic Account below for further details).

The aim of our research was to study the relationships among the species of 32nd *Onthophagus* group applying the combined phylogenetic approach to a dataset of discrete and continuous morphological characters. Once the phylogenetic relationships within the group were clarified, the evolutionary and biogeographic patterns of these species were examined to define which speciation processes led to the current biogeographical ranges, and how. Finally, the taxonomic status of the 32nd group was thoroughly reassessed according to the former phylogenetic results to formalize any reclassification at the generic and specific level.

MATERIAL AND METHODS

To explore the relationships among the *Onthophagus* species of the d'Orbigny 32nd group, a combined phylogenetic approach was applied on morphological data (discrete and continuous characters, see below) based on the external and internal features. This method was selected being it extremely versatile. Formerly, the quantitative data could not be employed "just as they were" in phylogenetic analysis, but were discretized during the analysis (Goloboff *et al.*, 2006; Gold *et al.*, 2014). Thus, the recent formalization of the combined approach (Goloboff & Catalano, 2010; Catalano *et al.*, 2010) has opened up huge opportunities for the use of extremely diverse characters that were hitherto inapplicable.

The assembled dataset included seven ingroup taxa (i.e., the six already-known species, plus a new species herein described), and one outgroup taxon, *Digitonthophagus bonasus* (Fabricius, 1775).

Material examined

We examined more than fifteen hundred specimens that were lent to us by the following Institutions:

- BMNH Natural History Museum, London, UK
- IRSNB Institut Royal des Sciences Naturelles de Belgique, Bruxelles, Belgium
- LACM Natural History Museum of Los Angeles County, Los Angeles, USA
- MCST Museo Civico di Storia Naturale, Trieste, Italy
- MHNL Musée des Confluences, Lyon, France
- MNCN Museo Nacional de Ciencias Naturales, Madrid, Spain
- MNHN Muséum National d'Histoire Naturelle, Paris, France
- NHMW Naturhistorisches Museum, Wien, Austria
- NMPC Narodni Muzeum v Praze, Prague, Czech Republic
- TMSA Ditsong National Museum of Natural History, Pretoria, South Africa
- ZMHB Museum für Naturkunde der Humboldt-Universität, Berlin, Germany
- ZSM Zoologische Staatssammlung, München, Germany

and by the following private collectors: E. Barbero (EBCT - Torino, Italy), I. Bonato (IBCT - Torino, Italy), T. Branco (TBCP - Porto, Portugal), I. De Dinechin (IDCL - Lyon, France), M. Dierkens (MDCL - Lyon, France), O. Montreuil (OMCF - Fleury-les-Aubrais, France), P. Moretto (PMCT - Toulon, France), and P. Walter (PWCM - Montségur, France).

Taxa coding

The species, named from now on according to the taxonomic rearrangement proposed below (see the Taxonomic Account), were coded as follows: *Hamonthophagus acutus* as AC, or red colour, *H. bituberculatus* as BI, or blue colour, *H. depressus* as DE, or orange colour, *H. fallax* as FA, or purple colour, *H. laceratus* as LA, or green colour, *Morettius pallens* as PA, or teal colour, and *M. utete* as UT, or burgundy colour.

Morphological analysis

Various anatomical parts (i.e., head, mouthparts, pronotum, fore legs, elytra, male and female genitalia) were selected to assess inter and intraspecific morphological differences (Barbero *et al.*, 2009, 2011; Roggero *et al.*, 2015). The mouthparts and genitalia of both sexes were dissected and treated following the methods usually employed to prepare slides in Scarabaeoidea (Barbero *et al.*, 2003). Then, images of internal and external structures were captured using a Leica® DFC320 digital camera connected to a stereoscopic dissecting microscope (Leica® Z16Apo).

The nomenclature of the anatomical traits adopted in this study follows that used in Palestrini (1992), Tarasov & Solodovnikov (2011), and Roggero *et al.* (2015, 2016). The anatomical traits were examined, and a set of distinctive characters (N = 26) was identified and used to build a discrete data matrix. Usually, a large number of features concur in characterizing taxa. Some could be quantified (see below for the novel approach employed here), but others cannot, and must necessarily be treated using a qualitative approach.

The geometric morphometric (GM) approach was here employed to evaluate phylogenetic patterns of diversification according to Gold *et al*. (2014). To test inter- and intraspecific shape variation within the 32nd group species, both landmark and semilandmark methods were applied (Fig. S1 - Appendix 1), choosing the best configuration to capture the overall shape variation of the head (19 points), the epipharynx (17 points), the mentum (22 points), the pronotum (11 points), and the right elytron (14 points). Each landmark configuration was sampled as implemented in tpsDig2 v2.27 (Rohlf, 2016a) and tps Util v1.69 (Rohlf, 2016b). The sampled datasets were then separately analyzed by tpsSmall v1.33 (Rohlf, 2016c) and tpsRelw v1.65 (Rohlf, 2016d) to evaluate the reciprocal relationships among the species, retaining for further analyses the Procrustes distances matrices (PD), the relative warp values (RWs), and the aligned configurations (AL). For each structure, the scatterplots of the RWs and the minimum spanning trees (MST) were built using NTSYS v2.21 (Rohlf, 2012).

Phylogenetic analysis

To clarify the phylogenetic relationships among the *Onthophagus* 32nd group species, a combined data matrix (Table S1 - Appendix 2) was built, merging together discrete and

continuous characters (N = 192). The aligned configurations of each anatomical trait were chosen to avoid the use of the principal components (PCs) of shape (i.e., the RWs, see above) as characters of phylogenetic analysis, as stated by Adams *et al.* (2011). The arbitrary value of 1 was added to the quantitative data employed for the phylogenetic analysis, since TNT (Goloboff *et al.*, 2003, 2006, 2008) cannot analyze negative numbers (Smith & Hendricks 2013; Gold *et al*. 2014). The outgroup method was chosen to root the trees, with *Digitonthophagus* as the root following T. Branco (*pers. comm.*) who has hypothesized that the 32nd group is phylogenetically well-separated from the *Onthophagus* groups, and probably closer to other Onthophagini genera. Also in Roggero *et al.* (2016) the species of 32nd group were closer to *Digitonthophagus* and allied taxa than to the other *Onthophagus* species.

To estimate the relationships among the species, a phylogenetic analysis was conducted using the combined approach in TNT (Goloboff *et al.*, 2003, 2008), where each morphometric character was used as a continuous numerical variable, and the quantitative and qualitative characters were treated as separate blocks in the linear parsimony analysis (de Bivort *et al.*, 2010, 2012; Clouse *et al.*, 2010). Implicit enumeration, traditional search and new technology search were run as implemented in TNT following Sharkey *et al.* (2012). The TNT script "stats.run" was then used to evaluate the tree statistics. Relative nodal support values were determined using bootstrap, jackknife and symmetrical resampling with 1,000 iterations, as implemented in TNT (Sharkey *et al.*, 2012). The resulting trees were then drawn by FigTree v1.4.2 (Rambaut, 2014).

Biogeographical analysis

Specific ranges were identified by employing only material herein examined. Each locality was georeferenced, and coordinates were used to build the digital maps of the distribution for each species (see Appendix 3 for the list of the localities) in the GIS environment through QGis v2.16 (QGIS Development Team, 2016). Collection localities were then grouped together in eight macroareas (Fig. 1) according to the terrestrial ecoregions proposed by Olson *et al.* (2001), and to the phytogeographical areas proposed by White and Leonard (1991). The distribution data of the species were then summarized in a presence/absence matrix that was employed for the dispersal-

vicariance analysis as implemented in RASP (Statistical Dispersal-Vicariance Analysis method, Yu *et al.*, 2010a, 2010b), with the maximum number of ancestral areas set equal to 2.

The Vicariance Inference Program (VIP, see Arias *et al.*, 2011) was employed to perform the Spatial Analysis of Vicariance, a method focused on the identification of disjoint (i.e., vicariant, or allopatric) distributions related to the formation of new barriers among sister groups instead of finding the ancestral areas, as in the traditional phylogenetic biogeography. In the analysis, sympatric speciations can also be highlighted since they occur whenever the species distributions overlap. In the VIP approach, the node removal is connected with dispersal, identifying any speciation that cannot be explained by the current reconstruction, and no process can be associated with the "geography of the distribution" of these species. In this framework, the georeferenced distribution data were used as spatial information, while the phylogenetic tree from TNT analysis furnished the phylogenetic information required by VIP. According to Ferretti *et al.* (2012), the analysis was performed using a grid of 1.5x1.5, selecting the Von Neumann neighbourhood and a maximum fill of 1. The default parameters of VIP were employed for the heuristic search, with 100,000 iterations, and the Bremer support was then calculated for each vicariant node. The hypothetical (heuristic) barriers among clades were represented on the maps by Voronoi lines (Arias *et al.*, 2011).

The results from VIP were then compared to the former RASP results, to test the hypothesized biogeographic history.

RESULTS

Morphological analysis

The detailed examination of the mentum, genitalia of both sexes, legs, head, pronotum, and elytra led to the identification of 26 qualitative characters (see the Characters List below), but some features could not be properly defined by a descriptive delineation of the characters. The complexity of anatomical shape was often better appraised by a quantitative approach (such as that provided by GM) than by a qualitative one, so the

mentum, head, pronotum, and elytra were also examined from a quantitative point of view. The epipharynx (Fig. 2) was instead examined only by the quantitative approach, which can better highlight even the most subtle shape variations.
The discrete and continuous data (characters 1-26 and 27-192, respectively, but see the Characters List below) were then used to build the combined matrix for the phylogenetic analysis (Table S1 - Appendix 2).

For each dataset, the relationships among the species were examined to test the morphological pattern of diversification applying GM methods. For this, the overall shape variation of each structure was studied separately and the amount of specific difference was quantified and employed in the subsequent phylogenetic analysis (linear parsimony, see below). The congruences/divergences of the identified patterns of morphological variation were also explored at the specific and generic levels.
Only the plots of the specimens actually employed to build the phylogenetic matrix of the aligned data were shown for each structure (Figs. 3-4). In each dataset, the typical material (if available) was included, but when types could not be found, topotypical material was selected. On each plot, the MST (built from the Procrustes distances matrix) was added to provide a more thorough insight into the differences among the species.

In the plot of the two first RWs of the head, well-defined groups were identified, and the species showed clearly differentiated patterns. The variance explained by the first two RWs was 84.74% for the head. The outgroup taxon is more similar to the group UT-PA than to any other species, and the five species included in *Hamonthophagus* share similar patterns of shape variation, with LA more closely related to BI than to the group UT-PA. Besides, according to our results, the head is a structure characterized by two distinctive patterns, allowing us to easily separate the genera, but also the species within each genus can be identified. Examining the deformation grids of RW_1 (Fig. 3), the head was clearly more rounded and the notch on the fore margin was absent (or greatly reduced) in OUT and in UT-PA, while the head was more elongated and deeply notched in the *Hamonthophagus* species. The deformation grids of the RW_2 (Fig. 3) showed a similar pattern, in which the head was broader and shorter in AC-DE and

(partially) in FA, elongating gradually in BI and LA on the one hand, and in UT-PA and OUT on the other.

The shape variation of the pronotum mainly accounted for distinct patterns at the generic level (Fig. 3) in which OUT, the *Hamonthophagus* species, and the *Morettius* species formed three well-separated groups. However, it is noteworthy that in the plot (Fig. 3) LA is separated from the other *Hamonthophagus* species, while OUT is nearer to *Hamonthophagus* than to UT-PA. The deformation grids of the RW_1 showed two distinct patterns, characterized by marked differences in the development of the fore angles, and in the more or less marked posterior expansion of the pronotum. The deformation grids of RW_2 showed instead differences in the lateral expansion of the pronotum, which is slightly rounded in *Hamonthophagus*, broadly more expanded in *Morettius*, and clearly extending outward in the central part in OUT. Here, the variance explained by the first two RWs was 79.96%.

Noteworthy differences were found mostly at the generic level in the elytron, and again three distinct groups were evident on the plot (Fig. 3), with 89.71%. of the variance explained by the first two RWs. The deformation grids of RW_1 highlighted marked differences in the elytron shape, with a more slender and narrow elytron in UT-PA, and a broader one in OUT, with *Hamonthophagus* well-separated and placed in an intermediate position. Also, the deformation grids of RW_2 demonstrated two distinct patterns, in which UT-PA-and OUT showed an elytron more elongated than *Hamonthophagus*. As before, LA is the species nearer to OUT, although the most secluded species appears to be FA. On the other hand, UT and PA seem to be more closely related to *Hamonthophagus* than to OUT.

For the mentum, the variance explained by the first two RWs was 84.37%, showing marked differences at the generic and specific levels in the plot (Fig. 3). The groups were clearly differentiated, with OUT well-characterized and isolated, while UT-PA showed a more marked similarity with *Hamonthophagus*. UT and PA had an ostensibly different mentum, although they remained more closely related to each other than to any *Hamonthophagus* species. Again, LA was the most secluded *Hamonthophagus* species,

and partly replicated the situation already evident in the other structures. The deformation grids of RW_1 (Fig. 3) showed conspicuous variations at fore and hind margins, that were more or less deeply notched in OUT and *Hamonthophagus* respectively. Also, the deformation grids of RW_2 (Fig. 3) showed distinct patterns of shape variation with the mentum more squared on the sides in *Hamonthophagus*, and far more rounded and expanded in OUT, with UT-PA in an intermediate position. On the whole, the mentum proved a rather interesting structure, characterized by obvious and marked differences at the specific and generic levels.

In the plot of the epipharynx (Fig. 4, with 72.04% of the variance explained by the first two RWs), some particularly interesting results were found. Roggero *et al.* (2015) have already pointed out that this structure is a very useful tool for taxa discrimination at the specific and generic levels in Scarabaeidae. Distinct groups are here plainly manifest, with OUT well-separated from the other species, UT-PA closely related, and *Hamonthophagus* forming a third group in which the majority of the species were sorted. LA is clearly distinct from the other *Hamonthophagus* species, but nevertheless remains more closely related to them than to UT-PA. The deformation grids of RW_1 (Fig. 4) showed well-defined patterns of variation, particularly on the fore margin (more notched in OUT), the tormae of the haptomerum area (larger in OUT), and the proplegmatium (more downwardly arched in *Hamonthophagus*). The deformation grids of RW_2 accounted mainly for variations of the supporting sclerotized structures (i.e. the tormae), such as the crepis (shorter and larger in *Hamonthophagus* than in UT-PA) and the tormae of the haptomerum (higher in UT-PA, and LA).

All the structures examined by GM methods provided useful information about the patterns of variation among these species, and contributed in elucidating their relationships based on morphological differences. Thus, the aligned configurations of head, pronotum, right elytron, mentum and epipharynx were employed to build the matrix for the phylogenetic analysis without converting them into linear values.

Characters List

(Figs 2-12)

1. Head: (0) uniform punctuation in clypeal and frontal parts; (1) punctuation of clypeal part strongly differing from the frontal one.

2. Frontal carina: (0) elongate; (1) intermediate; (2) short.

3. Pronotum length: (0) greater than 2.5mm; (1) smaller than 2.5mm.

4. Pronotum width: (0) greater than 4.5mm; (1) smaller than 4.5mm.

5. Pronotum, punctuation: (0) absent; (1) present.

6. Elytral interstria with punctuation: (0) almost inapparent, with small granules; (1) thick and rasping, with medium-sized granules; (2) more or less large, but always strong, with small and medium granules.

7. Elytral stria (Fig. 5): (0) larger than the points; (1) as large as the points; (2) narrower than the points.

8. Pygidium (Fig. 6) **in males M, width/height ratio:** (0) less than 1.60; (1) more than 1.60.

9. Pygidium, punctuation constituted by: (0) few, small and shallow points; (1) large and strong, but scattered points; (2) large, strong and thick points.

10. Fore tibia in males, between the first and the second tooth a secondary serration: (0) inapparent; (1) simple; (2) double.

11. Fore tibia in males, between the second and the third tooth a secondary serration: (0) inapparent; (1) with two small denticles; (2) with one small denticle.

12. Fore tibia in males, after the third tooth a secondary serration: (0) inapparent; (1) with one small denticle.; (2) with two small denticles.

13. Fore tibia in females, between the first and the second tooth a secondary serration: (0) inapparent; (1)) with one small denticle; (2) with two small denticles.

14. Fore tibia in females, between second and third tooth a secondary serration: (0) inapparent; (1 with one small denticle; (2) with two small denticles.

15. Fore tibia in females, after the third tooth a secondary serration: (0) inapparent; (1) with one small denticle.

16. Phalloteca, apices of paramers (Fig. 7)**:** (0) greatly reduced; (1) well-developed.

17. Paramers, finger-shaped ventral expansion (Fig. 7)**:** (0) developed; (1) reduced, almost inapparent.

18. Paramers, the finger-shaped expansion inserted (with respect to the paramers base): (0) high; (1) low.

19. Endophallus (Fig. 8) **constituted by:** (0) 2 sclerites; (1) more than 2 sclerites.

20. Endophallus, primary sclerite with a longitudinal development (Fig. 8)**:** (0) squat and short; (1) elongate and narrow.

21. Endophallus, primary sclerite carrying at base (Fig. 8)**:** (0) a convoluted expansion; (1) an evident hook.

22. Endophallus, primary sclerite apical part (Fig. 8)**:** (0) little elongate, linear; (1) very elongated and sinuate.

23. Receptaculum seminis, at base (Fig. 9)**:** (0) large; (1) narrow.

24. Vagina, sclerotization (Figs. 10-11)**:** (0) present; (1) absent.

25. Vagina, sclerotization (Figs. 9-10)**:** (0) groove-shaped, with part 1 inapparent; (1) funnel-shaped, with part 1 large and deep; (2) funnel-shaped with part 1 deep and narrow.

26. Mentum, second palpus (Fig. 12)**:** (0) narrow, sub-cylindrical; (1) expanded, and rounded.

27-192. Aligned configurations (quantitative data) of epipharynx (27-60), mentum (61-104), head (105-142), pronotum (143-164), and right elytron (165-192) (Figs. 3-4).

Phylogenetic analysis

The linear parsimony analysis on the combined data matrix always gave the same single tree (Fig. 13), in which two distinct clades are present, one including UT and PA, and the other including all the other species. The results thus confirmed that the 32nd group is not a homogenous taxon. The *Morettius* clade is supported by resampling values of 85/87/94, while the *Hamonthophagus* clade is supported by resampling values of 61/83/78 for the Standard Bootstrap, Symmetrical Resampling, and Jackknife respectively. It is also noteworthy that *H. laceratus* is the most separated species in the *Hamonthophagus* clade, with high support values, endorsing the observations from the geometric morphometrics analysis. The following node also shows high support values, while the last node has much lower support values (Fig. 13), since the species of the

clade AC, FA and BI are strictly interrelated, although BI and FA are closer to each other than to AC.

Biogeographical analysis

The *Hamonthophagus* species were characterized by a wide distribution (Fig. 14) covering at least two macroareas, while *Morettius* species were characterized by more reduced distributions. The georeferenced localities were mapped onto the terrestrial ecoregions, giving clear differences in the species distributions. While AC is present in the more xeric areas, extending only patchily in the savannah ecoregion, BI can be considered a typical savannah species, with a greatly-extended distribution over the entire central area of the Afrotropical region. Also DE and FA are essentially savannah species, with a more southerly distribution than BI, and a much reduced presence in desert areas (Fig. 14). The distribution of LA, covering the whole NE Afrotropical region is also characterized by a prevalent savannah distribution, never reaching the alpine steppe or the rain forest ecoregions.

The results of RASP (Fig. 15) gave a reconstruction of ancestral areas characterized by three vicariant (green ring) and six dispersal (blue ring) events. At each node, a unique optimal distribution was identified, except for the nodes 10 and 13 in which two equiprobable alternatives were recognized, leading on the whole to four different reconstructions: 1) node 10: DE, and node 13: AD; 2) node 10: DE, and node 13: CD; 3) node 10: DF, and node 13: AD; 4) node 10: DF, and node 13: CD. A vicariant event was identified at node 15, in which the Oriental and Afrotropical clades were separated. In the following nodes (Fig. 15), only dispersal events were allowed, with D as an ancestral area. For the clade UT-PA, a vicariant event was evident, with PA being present in AC, and UT in D. For the clade AC-BI-FA, a vicariant event was obtained at Don the ancestral areas (BI-FA). On the basis of these results, it can be therefore hypothesized that these species diversified in D, then extended eastwards (BI, and LA) and southwards (FA, DE, and AC).

The VIP analysis produced a single possible reconstruction, identifying 3 disjunct sister pair (vicariant) nodes and 3 node removals (dispersal). The 1st vicariant node (node 8, Fig. 16) corresponded to the split of the *Morettius* species from the *Hamonthophagus* species, and the heuristic barrier (shown in red, Fig. 16a) separated A from B-G areas. The 2nd vicariant event (node 9, Fig. 16) resulted in the separation of PA from UT with a hypothetical barrier (shown in green, Fig. 16b) running along the Rift Valley and reaching westward to the Namibian Coast, thus splitting the A-C areas from the D area. The 3rd vicariant event (node 12, Fig. 16) took place between AC and the clade FA/BI, with a possible vicariant barrier through the A-D and E-G areas respectively (shown in blue, Fig. 16e). In the reconstruction, three sympatric speciations were evident in the nodes 10, 11, and 13 (Fig. 16) where for each there was a high species overlap for the *Hamonthophagus* species (Fig. 16c,d and f).

Taxonomic account

Genus *Hamonthophagus* gen. nov.

Type species. *Onthophagus bituberculatus* Olivier, 1789.

Included species. At present five Afrotropical medium size species (Figs. S2-3 - Appendix 4) can be included in the genus *Hamonthophagus* **gen. nov.**, namely: *H. acutus* (d'Orbigny, 1908), *H. biturberculatus* (Olivier, 1789), *H. depressus* (Harold, 1871), *H. fallax* (d'Orbigny, 1913), and *H. laceratus* (Gerstaecker, 1871).

Diagnosis. The species included in the genus *Hamonthophagus* are strictly allied, and share a combination of characters that distinguishes them from the other Onthophagini: the anterior margin of the clypeus mostly sinuate and bidentate, and both head carinae poorly developed (i.e., slightly marked frontal carina and simple vertex carina). The granulo-punctuate pronotum is not very convex, and has evident anterior angles with divergent apices, that are inferiorly prolonged to strong prosternal carina. Head and pronotum are usually black or dark brown. The elytra are flat, narrowed backwards, with marked striae and interstriae, extremely variable in coloration, ranging from evenly black to yellow with a discal dark spot.

Sexual dimorphism was shown in the protibia (carrying a tooth on the inner margin only in males), and pygidium (far more developed in males than females), as is common in Onthophagini.

Epipharynx. The epipharynx (Fig. 2) is characterized by a rounded anterior margin gently notched in the middle, abundant and widespread acropariae, and well-developed corypha. The pubescence of the haptomerum is thick, the chaetopariae are almost rectilinear, constituted by short and dense setae. The anterior epitorma is longitudinal and narrow, the proplegmatium well-sclerotized and arched, the apotormae are present, and the crepis is small, sharp and left-turned. The dexiotorma and laeotorma are slightly asymmetrical.

Male genitalia. The male is characterized by a medium size phallotheca (or aedaegus, Fig. 7) with symmetrical parameres, and well-developed apices, carrying ventrally a symmetrical expansion. The membranous internal sac (or endophallus, Fig. 8) carries a hook-shaped and well-sclerotized primary sclerite, and some small accessory sclerites.

Female genitalia. In females, an asymmetrical, well-sclerotized funnel-shaped area is evident in the vagina (Figs. 9-10), and is perhaps the most obvious character of the genus. The membranaceous and plurisinuate infundibulum is barely visible, being basally located at a very low position, just on the oviductus. The receptaculum seminis (Figs. 9-10) is curved in distal third, more enlarged at base, and tapering to apex, with a large desclerotized area medially.

Specific diagnosis. The *Hamonthophagus* species can be distinguished on the basis of some external features, as the body pubescence, the elytral striae and the punctuation of pronotum and pygidium. Clear differences in shape were underlined by the geometric morphometrics analysis of head, pronotum, elytron and mentum (see above). Marked differences can also be highlighted by the analysis of the epipharynx (always, according to the geometric morphometrics approach) and genitalia.

The pubescence covering the body is constituted by thick, ochreous, and truncated setae that are short in *H. depressus*, *H. acutus* and *H. fallax*, and longer in *H. bituberculatus*, while in *H. laceratus* the setae are very elongate, thinner and not truncated.

The pronotum has a characteristic punctuation with varyingly sized, closely spaced, double points often carrying a hook-shaped granule never covering the point. While the points are usually dense (but excluding *H. laceratus*), in *H. bituberculatus* only the

larger points bear the minute and flat granules, while in *H. acutus, H. fallax* and *H. depressus,* the majority of the evident points carry well developed and thick granules. *Hamonthophagus laceratus* is characterized instead by sparse and superficial points, with very minute and scattered granules.

The elytral striae are constituted by a very narrow line with larger points, except *H. laceratus*, where there are instead large striae with small points. Rasping, dense small setigerous points are present on the interstriae, and in *H. acutus* and *H. bituberculatus* the granules are small, while in *H. depressus* and *H. fallax* they are broader and evident. Again, in *H. laceratus* the points are rade, and almost inapparent, with few, very small granules. *Hamonthophagus fallax* usually carries an evident testaceous dot on the proximal sides of the elytra, that are distally narrower than those in *H. depressus*.

In *H. acutus,* the pygidium is covered by superficial points and evident, roundish and small granules, while in *H. depressus* and *H. fallax* the dense, large setigerous points are without granules on the disc, carrying sometimes rough points only on the sides. Besides, the latter species both have an evident and cerebroid microsculpture on the surface, that in *H. acutus* is less marked. The pygidium of *H. bituberculatus* has an opaque, smooth surface with few, scattered, shallow points (sometimes with minute granules), but an evident, very thick microsculpture. Also in *H. laceratus,* the pygidium is almost smooth, with an evident microsculpture, with only few and sparse points lacking granules.

The fore margin of the epipharynx (Fig. 2) is only weakly notched in the middle in *H. acutus*, while in *H. bituberculatus, H. depressus* and *H. fallax* the notch is V-shaped, more marked and large. In *H. laceratus* the fore margin is slightly more squared that in the other species. The apotormae are less developed in *H. bituberculatus* and *H. laceratus* than in the other species. The crepis is more reduced in *H. acutus* and *H. fallax*. The medial triangular sclerotized area of the proplegmatium is far shorter in *H. fallax* than in the other species. In *H. laceratus* the rear sclerotized part between the proplegmatium and crepis is much longer than in any other species.

In males, the paramers apices are elongate, large and only slightly hooked in *H. acutus H. bituberculatus* and *H. fallax,* and more slender in *H. depressus*. In *H. laceratus,* the parameres of the aedeagus are narrower than in the other *Hamonthophagus*, rounded at

apex and slightly downcurved. The small, rounded ventral expansion is well-developed mainly in *H. laceratus* (see Fig. 7 for the comparison among the species).

The primary lamella of the endophallus is elongate with a large hook at the base in *H. acutus, H. bituberculatus, H. depressus and H. fallax*, with small differences in the longitudinal development among these species. In *H. laceratus* the primary lamella is more peculiar, being tougher and half as long as in the other species, but always hook-shaped (see Fig. 8 for the comparison among the species).

These species can also be easily identified by the shape of the peculiar asymmetrical, funnel-shaped sclerotization of the vagina that shows a characteristic and differentiated development in the five species (see Fig. 10 for the comparison among the species).

General remarks. No preimaginal stages have been described so far.

Distribution. The genus *Hamonthophagus* is distributed in arid and savannah Afrotropical Regions (Fig. 14).

Etymology. The new genus was named after the Latin word *hamo*, = hook with reference to the characteristic shape of the primary lamella of the internal sac.

***Hamonthophagus acutus* (d'Orbigny, 1908: 171)**

(Figs. 2, 7, 8, 10)

Type material. NAMIBIA [Sud-Ouest africain allemand]: Okahandja [MNHN]. Paralectotypes: BOTSWANA: lake Ngami [MNHN]. DEMOCRATIC REPUBLIC OF CONGO: [Tanganyika,] région de Mpala [MNHN]. MALAWI: Malawi Lake [= Nyassa] [not located]. NAMIBIA: Salem [not located]. SOUTH AFRICA: Eastern Cape province [= Cafrerie] [MNHN]. For the morphological account, please refer to the original description.

Geographic distribution (Fig. 14). The species distribution surely comprises Namibia, SW Botswana, and NW South Africa (see Appendix 3 for a detailed list of the localities). Besides, in the type series d'Orbigny (1908) included also material from the Tanganika area (Democratic Republic of Congo), and Nyassa (i.e., Malawi). The former specimen was reported in the Collection Oberthur, MNHN, and the latter was reported in "coll. du British Museum" (now BMNH) where, however, it has not been traced (M. Barclay, *pers. comm.*). Neither specimen could be examined by us. Since no other collection data from these areas were found within the studied material, these records

were here regarded as uncertain until further confirmation. Also, a specimen from the MNHN labelled as "Sénègal provenance tres douteuse" was not included in the present analysis.

***Hamonthophagus bituberculatus* (Olivier, 1789: 131)**

(Figs. 2, 7, 8, 10)

Synonymy.

Onthophagus discoideus (Olivier, 1789:171) *teste* Harold 1880

Type material. At present, the typical material of *H. bituberculatus* could not be found. Although various materials of the Olivier collection were traced in several museum collections over the years (Bragg, 1996; Staines & Whittington, 2003; Gültekin & Korotyaev, 2011), most specimens are still missing. The type material of this species was collected from "Senegal" by Geoffroy de Villeneuve, as well as its synonym *O. discoideus* (that was recorded also from Gorée Island). Since the type material of this species could not be located at present, no lectotype could be designed here. For the morphological account, please refer to the original description.

Geographic distribution (Fig. 14). The species is widely distributed in the whole sub-Saharan area (Benin, Burkina Faso, Eritrea, Ethiopia, Gambia, Ghana, Guinea, Guinea Bissau, Ivory Coast, Mauritania, Niger, Nigeria, Senegal (the type locality), Sudan, and Togo), and in Central and Eastern Africa (Central African Republic, Chad, Democratic Republic of Congo, Gabon, Kenya, Republic of Congo, and Uganda) extending eastwards and southwards toward Tanzania and Malawi (see Appendix 3 for more details). The species is also recorded from Cairo (Egypt, Schatzmayr, 1946; Baraud, 1985) and Arabia (Paulian, 1980), but the data need to be confirmed. Accidental introduction is reported in Antilles (Martinique), where an anthropic cause was hypothesized to explain these findings (Matthews, 1966; Chalumeau, 1983).

***Hamonthophagus depressus* (Harold, 1871: 116)**

(Figs. 2, 7, 8, 10)

Synonymy.

Onthophagus laceratus Peringuey 1901 nec Harold

Onthophagus carteri Blackburn, 1904: 147 *teste* Cartwright 1938

depressus var. *marmoreus* d'Orbigny 1904: 309

Type material. Lectotype here designated: (male) SOUTH AFRICA: [Caffraria =] Eastern Cape province [ZMHB]. For the morphological account, please refer to the original description.

Geographic distribution (Fig. 14). The species was originally described from South Africa, Caffraria (now, Eastern Cape Province), but shows a wide distribution (the full list of the localities can be found in Appendix 3) extending in a large part of the Afrotropical region (Angola, Botswana, Burundi, Democratic Republic of Congo, Kenya, Malawi, Mozambique, Namibia, South Africa, Tanzania, Zambia, and Zimbabwe). Accidental introduction in Madagascar, Mauritius, USA (Florida, Georgia and South Carolina), and Australia (New South Wales and Queensland). Howden & Cartwright (1963) reported that specimens were collected at light in Georgia by Fattig. In the USA, *H. depressus* has been recorded in Georgia, SW South Carolina and Florida (Hunter & Fincher, 1996; Hoebeke & Beucke, 1997; Evans, 2014), with a scattered distribution, since 1937 (Cartwright, 1938). The species was unintentionally introduced in Australia surely before 1900 (Matthews, 1972; Woodruff, 1973), when Blackburn (1904) described *H. depressus* specimens as a new species naming it *O. carteri*. This species was later properly identified as *O. depressus* by Arrow (see Cartwright, 1938). It is likely that the first introduction in Australia could be localized to the area near Sydney, from where it began to expand its range starting from 1941 (Matthews, 1972; Woodruff, 1973).

***Hamonthophagus fallax* (d'Orbigny, 1913: 471)**

(Figs. 2, 7, 8, 10)

Type material. Lectotype here designated: (male) MALAWI: [Nyassa Zomba haut Chiré=] Zomba, Shire river upper course, Malawi Lake [MNHN]. Paralectotype: (female) TANZANIA [=Afrique Or Alem]: Dar-es-Salaam [MNHN]. For the morphological account, please refer to the original description.

Geographic distribution (Fig. 14). The species has been described from Malawi and Tanzania, and at present is recorded from Botswana, Burundi, Democratic Republic of Congo, Kenya, Malawi, Namibia, Tanzania, and Zambia. The record from Graaf-Reinet

(Eastern Cape province, South Africa) is surely very interesting, but needs to be confirmed by further records. In Appendix 3, a detailed list of the localities is given.

***Hamonthophagus laceratus* (Gerstaecker, 1871: 50)**

(Figs. 2, 7, 8, 10)

Synonymy.

Onthophagus laceratus subsp. *benadirensis* Müller 1942: 82

Type material. Lectotype here designated: (male) TANZANIA: Zanzibar [ZMHB]. Paralectotype: (female) same locality [ZMHB]. The subspecies *benadirensis* from Mogadishu area (Somalia) was examined and no marked differences were evident from the nominal species. For the morphological account, please refer to the original descriptions.

Geographic distribution (Fig. 14). The species was described from Zanzibar, and shows a wide distribution extending in Burundi, Democratic Republic of Congo, Ethiopia, Kenya, Somalia, Sudan, and Tanzania (see Appendix 3 for the full list of the localities).

Genus *Morettius* gen. nov.

Type species. *Onthophagus pallens* d'Orbigny, 1908

Included species. *M. pallens* (d'Orbigny, 1908), and *M. utete* **sp. nov.**

Diagnosis. The species of the genus *Morettius* (Fig. S3 - Appendix 4) are characterized by the mostly rounded and only slightly notched anterior margin of the clypeus, and the pronotum covered by granules, sometimes mixed to points. The pygidium is always smooth, with some rade points. The species show a moderate sexual dimorphism in the fore tibiae, and the pygidium is larger in males than in females.

Epipharynx. The epipharynx (Fig. 2) fore margin is arched, with a largely V-shaped notch in the middle. The corypha is reduced, the chaetopariae are arched with short, thick, and almost equal length setae. The pubescence of the haptomerum is dense. The proplegmatium is subequal on the whole length, with the posterior triangular sclerotization reaching at least as much or more than half of the length of the anterior epitorma, that is rectilinear, well-sclerotized and thin. The base of the triangular

sclerotization reaches the small, thick and upward-turned apophyses. Laeotorma and dexiotorma are symmetrical, short and stout. Pternotormae are well-sclerotized, the crepis is short but evident, with a sharp apex. The plegmatic area is visible.

Male genitalia. Only the male genitalia of *M. pallens* could be examined. The phallobase (Fig. 7) is short, only slightly arched, slender, of equal size along the whole length. The parameres are symmetrical, and squared, with a small tip at the apex, and a small, rounded protrusion ventrally. The internal sac (Fig. 8) is membranous, with various well-sclerotized parts greatly differing from the *Hamonthophagus* species.

Female genitalia. The female genitalia are very peculiar (Fig. 11), since the vagina of both species is entirely membranous, and no sclerotization is present at all. Furthermore, the infundibular tube is lowered as in *Hamonthophagus*, but here an expanded portion is identifiable in the central part of vagina, which is differently shaped in the two species. The receptaculum seminis is sickle-shaped, namely slim, arched, and apically sharp (Fig. 9).

Specific diagnosis. These species can be easily distinguished on the basis of external morphology, epipharynx and female genitalia.

The pronotum in *M. pallens* is covered by distinct rasping points mixed with smaller, yellow granules; the granules of the rasping points instead are large, darker than the background surface, and carry long, thick, and light yellow setae. The pronotum of *M. utete* is covered by only few rasping setigerous points with thin, yellow setae and many small granules, which are very thick, evenly coloured as the base, and without points. Elytral striae of *M. pallens* are as large as the points, being instead larger than the points in *M. utete*.

The smooth pygidium carries in *M. pallens* few, small, rade and deep setigerous points that are not granulated, and in *M. utete* only some large and superficial vanishing points without setae.

The epipharynx (see Fig. 2 for the comparison among the species) has the characteristic shape of the *Morettius* species, but can be distinguished from *M. utete* by the more developed apotormae, and the more slender laeotorma and dexiotorma.

In both species, the vagina is wholly desclerotized, but carries two globose symmetrical expansions that encircle the desclerotized and lowered infundibulum in *M. pallens*,

while in *M. utete* there is a single, large expansion (see Fig. 11 for the comparison among the species)

Since the male of *M. utete* is unknown, no comparison can be made between species.

General remarks. No preimaginal stages have been described so far.

Distribution. The genus *Morettius* is characterized by a disjoint distribution, being found in central west Africa, and southeastern Africa (Tanzania).

Etymology. The genus is named after our colleague, the French entomologist Philippe Moretto, who works extensively on African Scarabaeoidea.

***Morettius pallens* (d'Orbigny, 1908: 172)**

(Figs. 2, 7, 8, 11)

Type material. Lectotype here designated: (male) CHAD: Kiao-Kata, Moyen-Chari, south to Chad lake [=moyen Chari rives, Kiao-Kata] [MNHN]. Paralectotype: (female) same locality [MNHN]. For the morphological account, please refer to the original description.

Geographic distribution (Fig. 14). The species was reported from Cameroon, Chad, Nigeria (southern border) Republic of Congo, and Sudan (the collection localities were listed in Appendix 3).

***Morettius utete* sp. nov.**

(Figs. 2, 11, 17)

Etymology. The species was named after the collection locality.

Type material. Holotype: female, TANZANIA: Utete-Rufijikindwjivi [MHNL]. Paratypes: 2 females, same locality [MHNL] [EBCT].

Description

Male. Unknown

Female. Length: 6.1-6.6 mm. Head bronze, transverse (length/width ratio: 0,72), with maximum width just anteriorly to the eyes. Clypeus sinuate, with clypeal edge reddish. Clypeo-genal junction not sinuate. Frontal carina fine, weakly curved, placed at the mid-length of the head, short and low, occupying half of the interocular space. Surface markedly reticulate. Clypeus covered by flat and transverse granules, more or less merged. Genal granules large and round. Vertex unarmed, weakly concave, with round

and fine granules. Antennal scape normally shaped, not dentate or serrulate. Antennal club yellow.

Pronotum bronze, with hind angles bearing a bronze callus surrounded by a wide yellowish area covering more than the half of the pronotal length and prolonged narrowly on the sides to reach the anterior angles. Pronotal pubescence black and very short, only evident on the lateral edges. Pronotum unarmed, very weakly transverse (length/width ratio: 0.55). Base evenly curved, markedly bordered. Posterior angles not sinuate. Anterior angles strongly sinuate, sharply projected outwards. Surface reticulate. Area surrounding the callus not granulate; remaining pronotal surface entirely covered by small granules.

Elytra yellow with black symmetrical spots, one basal on the fifth interstriae, one on the first third of sixth and seventh interstriae, another four connected on the middle of the second to fifth interstriae forming a zig-zig pattern. Juxtasutural interstriae yellow-orange, darkened anteriorly. Basal carina of interstriae bronze. Pubescence yellow, very short and scattered, only evident posteriorly. Elytral ground reticulate. Interstriae bearing small yellow granules, arranged on the juxtasutural interstriae in a regular row. Interstriae weakly convex, basally carinate. Striae narrow, well-marked, yellow. Punctures of striae never wider than the striae. The seventh stria sinuate basally. Pygidium yellow almost smooth, finely microreticulate, with small, rare, hardly perceptible punctures. Base carinate.

Epipleura yellow. Sternal thoracic surface bronze, except for the base of propleurae bronze. Abdominal sternites yellow. Metasternal pubescence scattered, short and yellow.

Coxae yellow. Trochanters bronze. Femura yellow, apically bronze. Tibiae bronze, meso- and metatibiae apically yellowish. Tarsomeres weakly bronze. Pubescence yellow. Fore tibiae three-toothed. Tibial spur elongate, bent inward, apically rounded. Tarsi normally shaped.

Individual variation. Paratype: the wide posterior spot of the right elytra is extended on the sixth interstria. Spot of the scond interstria obviously longer than in the hotolypus. Seventh elytral stria only weakly sinuate.

Epipharynx (Fig. 2). See the above generic diagnosis.

Male genitalia. unknown

Female genitalia (Fig. 11). See the above generic diagnosis.

Geographic distribution (Fig. 14). The species is known only from the type locality.

Identification Keys

(Figs. S2-3 - Appendix 4)

1. Clypeal anterior edge mostly rounded and only slightly notched; pygidium smooth, sometimes with some fine and scattered points. In males (*M. pallens*), primary sclerite constituted by a well-sclerotized, almost spoon-shaped part and two less sclerotized laminar parts. In the female, vagina entirely membranous ……..…… *Morettius* (2)

1'. Clypeal anterior edge obviously bidentate; points of the pygidium fine or wide but never densely distributed. Hook-shaped and well-sclerotized primary sclerite of endophallus in male. Asymmetrical, well-sclerotized funnel-shaped area of the vagina in female. ……..……..…*Hamonthophagus* (3)

***Morettius* gen. nov**

2. Pronotum covered by distinct points carrying large granules darker than the surface covering the points mixed with smaller, yellow granules; the rasping points carry long, thick, light yellow setae ……..... *pallens* (d'Orbigny)

2'. Pronotum covered by many small, very thick evenly coloured granules; only few rasping setigerous points with thin, yellow setae …… *utete* **sp. nov.**

***Hamonthophagus* gen. nov.**

3. Pronotum black or dark brown with yellowish spots at the hind angles, and covered by sparse points, with very minute and rade granules ……. *laceratus* (Gerstaecker)

3'. Pronotum entirely black or dark brown, and covered by varyingly sized, closely spaced, dense double points often carrying hook-shaped granules .....…….…..... 4

4. Pronotum with simple, small points and larger points with minute and flat granules. Setae of the dorsal surface obviously longer than wide …….. *bituberculatus* (Olivier)

4'. Pronotum covered by granulate points. Setae of the dorsal surface largely as long as wide ……..……. 5

5. Pronotum evenly covered by granulate points. Pygidium covered by scattered but evident granules ……..……..……... *acutus* (d'Orbigny)

5'. Pronotum covered by large granulate points and few, very smaller simple points. Pygidium covered by rather large, more or less dense ocellate points ……..... 6

6. In males, apices of paramers elongate, large and only slightly hooked. In females, the sclerotized area asymmetrically developed with the apex on the right. Elytra black, with one or several testaceous, symmetrical, small patches ..……..…..… *fallax* (d'Orbigny)

6'. In males, apices of paramers more slender and pointed. In females, the sclerotized area well-developed and triangular-shaped. Elytra usually entirely black or, sometimes, dark brown ……. *depressus* (Harold)

DISCUSSION

The study of the d'Orbigny 32nd species group has been addressed by employing an innovative and very powerful approach. The combined phylogenetic method allowed us to handle together different morphological datasets of discrete and continuous characters, summarizing the modularized traits. Our first research goal was focused on testing how several trait configurations could be processed to gain quantitative data, and then utilized after being combined in a single matrix with the qualitative characters. The use of the quantitative approach often furnished more detailed information about various anatomical traits than the qualitative approach, also evidencing at its best the intra and interspecific differences of shape variation. Therefore, quantifying information can provide a more accurate dataset and allow more effective analysis of morphological characters.

On the whole, the results of the analyses concurred in highlighting a lack of phylogenetic homogeneity in the d'Orbigny 32nd species group, whereby the recognition of a generic-level divergence at the basal dichotomy of the tree was well-founded (Fig. 13).

The first genus was designated as *Hamonthophagus* and included the majority of the species (see the Taxonomic Account above), while the second one, namely *Morettius*,

included only two species, one of which was identified and described here (see the Taxonomic Account above). The two genera are clearly diversified on the basis of the shape of the epipharynx and genitalia of both sexes. These structure are characterized by marked complexity, evidencing the generic trends, since they usually constitute the synapomorphies founding the basal generic status. Additionally, while for the usefulness of the genitals in taxonomic research is well founded and undisputed (Eberhard, 2010a, 2010b, 2011), the epipharynx is still little used, although it has been extremely effective to define and separate even very challenging groups (Roggero *et al.*, 2015).

The age estimates for the African coprophagous radiations, as evaluated in recent analyses using four nuclear and mitochondrial DNA markers (Ahrens *et al.*, 2014), could also be applied to *Hamonthophagus* and *Morettius*. The scarab divergences were demonstrated in the calibrated Time-Tree showing scenarios closely related to a diversified pattern of herbivores (i.e., dung-producing mammal lineages). Such an evolutionary-ecological context could be allocated to the Miocene when the lineages should have radiated. This period was characterized by climatic changes that caused the spread of the savannah and the dominance of the dung-producing Artiodactyla (Wirta *et al.*, 2008; Sole & Scholtz, 2010). In this period, the ancestral generic lineages of most extant Scarabaeini/Onthophagini arose, and it is likely that *Hamonthophagus* and *Morettius* might be involved in these speciation processes, originating in the Eastern Central African area (area D, Fig. 1). Subsequently, these typically tunneling dung beetles split thanks to sequential migrations of herbivorous mammals (Monaghan *et al.*, 2007; Philips, 2011) across the entire continent towards the south and north, resulting in various and diversified dispersal events hypothesized in Fig. 18 for *Hamonthophagus*, with part of the group spreading south, and part extending northwards.

ACKNOWLEDGMENTS

This research was made possible thanks to grants from the Fondazione CRT, Research and Education section (Torino, Italy), and was also partly supported by the Italian Ministero dell'Istruzione, dell'Università e della Ricerca (MIUR). We are greatly

indebted to the museum curators and private collectors who kindly lent us their material. We are also very grateful to M. Barclay (BMNH, London) for the useful information on 32nd group type material. We want also to thank two anonymous reviewers whose comments and suggestions greatly contributed to improving our paper. We are very grateful to our colleague Dan Chamberlain, who kindly corrected the English text.

REFERENCES

Ahrens D, Schwarzer J, Vogler AP. 2014. The evolution of scarab beetles tracks the sequential rise of angiosperms and mammals. *Proceedings of the Royal Society B* 281: 20141470. DOI: 10.1098/rspb.2014.1470.

Adams DC, Cardini A, Monteiro LR, O'Higgins P, Rohlf FJ. 2011. Morphometrics and phylogenetics: Principal components of shape from cranial modules are neither appropriate nor effective cladistic characters. *Journal of Human Evolution* 60: 240-243.

Arias JS, Szumik CA, Goloboff PA. 2011. Spatial analysis of vicariance: a method for using direct geographical information in historical biogeography. *Cladistics* 27: 617–628.

Baraud J. 1985. Coléoptères Scarabaeoidea, Faune du nord de l'Afrique, du Maroc au Sinaï. *Encyclopédie Entomologique* 46: 1-652.

Barbero E, Palestrini C, Roggero A. 2003. *Revision of the genus Phalops Erichson, 1848 (Coleoptera: Scarabaeidae: Onthophagini).* Torino: Museo Regionale di Scienze Naturali.

Barbero E, Palestrini C, Roggero A. 2009. Systematics and phylogeny of *Eodrepanus*, a new Drepanocerine genus, with comments on biogeographical data (Coleoptera: Scarabaeidae: Oniticellini). *Journal of Natural History* 43: 1835–1878.

Barbero E, Palestrini C, Roggero A. 2011. *Tibiodrepanus tagliaferrii* - a new Afrotropical Drepanocerina species (Coleoptera: Scarabaeidae: Oniticellini), with notes on phylogeny and distribution of the genus. *Zootaxa* 2923: 27–47.

de Bivort BL, Clouse RM, Giribet G. 2010. A morphometrics-based phylogeny of the temperate Gondwanan mite harvestmen (Opiliones, Cyphophthalmi, Pettalidae). *Journal of Zoological Systematics and Evolutionary Research* 48: 294-309.

de Bivort BL, Clouse RM, Giribet G. 2012. A cladistic reconstruction of the ancestral mite harvestman (Arachnida, Opiliones, Cyphophthalmi): portrait of a Paleozoic detritivore. *Cladistics* 28, 582–597.

Blackburn T. 1904. Revision of the Australian Aphodiides, and descriptions of three new species allied to them. *Proceedings of the Royal Society of Victoria* 17: 145-181.

Bragg PE. 1996. Type specimens of Phasmida in the Nationaal Natuurhistorisch Museum, Leiden (Insecta: Phasmida). *Zoologische Mededelingen* 70: 105-115.

Catalano SA, Goloboff PA, Giannini P. 2010. Phylogenetic morphometrics (I): the use of landmark data in a phylogenetic framework. *Cladistics* 26: 539–549.

Chalumeau F. 1983. *Les Coléoptères Scarabaeides des Petites Antilles (Guadeloupe à Martínique). Taxonomie-Ethologie-Biogéographie*. Paris: Editions Lechevalier.

Clouse RM, de Bivort BL, Giribet G. 2010. Phylogenetic signal in morphometric data. *Cladistics* 27: 1-4.

Cartwright OL. 1938. A South African *Onthophagus* found in the United States. *Entomological News* 49: 114-115.

d'Orbigny H. 1908. Descriptions d'espèces nouvelles d'Onthophagides africains et notes synonimiques. *Annales de la Société Entomologique de France* 77: 65-208.

d'Orbigny H. 1913. Synopsis des Onthophagides d'Afrique. *Annales de la Société Entomologique de France* 82: 1-742.

Eberhard WG. 2010a. Evolution of genitalia – theories, evidence, and new directions. *Genetica* 138: 5-18. doi: 10.1007/s10709-009-9358-y.

Eberhard WG. 2010b. Rapid divergent evolution of genitalia. In: Leonard J., Cordoba A. eds. *The Evolution of Primary Sexual Characters in Animals*. Oxford: Oxford University Press, 40-78.

Eberhard WG. 2011. Experiments with genitalia: a commentary. *Trends in Ecology and Evolution* 26: 17-21. doi:10.1016/j.tree.2010.10.009.

905 Emlen DJ, Marangelo J, Ball B, Cunningham CW. 2005. Diversity in the weapons of
906 sexual selection: horn evolution in the beetle genus *Onthophagus* (Coleoptera:
907 Scarabaeidae). *Evolution* 59:1060-1084.
908 Emlen DJ, Szafran Q, Corley LS, Dworkin J. 2006. Insulin signaling and limb-
909 patterning: candidate pathways for the origin and evolutionary diversification of
910 beetle 'horns'. *Heredity* 97: 179-191.
911 Evans AV. 2014. *Beetles of Eastern North America*. Princeton (NJ): Princeton
912 University Press.
913 Ferretti N, González A, Pérez-Miles F. 2012. Historical biogeography of the genus
914 *Cyriocosmus* (Araneae: Theraphosidae) in the Neotropics according to an event-
915 based method and spatial analysis of vicariance. *Zoological Studies* 51: 526-535.
916 Gold MEL, Brochu CA, Norell MA. 2014. An Expanded Combined Evidence Approach
917 to the *Gavialis* Problem Using Geometric Morphometric Data from Crocodylian
918 Braincases and Eustachian Systems. *PLoS ONE* 9: e105793.
919 doi:10.1371/journal.pone.0105793.
920 Goloboff PA, Catalano SA. 2010. Phylogenetic morphometrics (II): algorithms for
921 landmark optimization. *Cladistics* 27:42-51. doi: 10.1111/j.1096-
922 0031.2010.00318.x.
923 Goloboff PA, Farris JS, Nixon KC. 2003. TNT: Tree Analysis Using New Technology.
924 Available at: http://www.zmuc.dk/public/phylogeny/TNT/ [through the Hennig
925 Society].
926 Goloboff PA, Farris JS, Nixon KC. 2008. TNT, a free program for phylogenetic
927 analysis. *Cladistics* 24: 774–786.
928 Goloboff, PA, Mattoni CI, Quinteros AS. 2006. Continuous characters analyzed as
929 such. *Cladistics* 22: 589-601. doi:10.1111/j.10960031.2006.00122.x.
930 Gültekin L, Korotyaev BA. 2011. *Lixus petiolicola* n. sp. from Northeastern Turkey and
931 *Lixus furcatus* Olivier: Comparative systematic and ecological study (Coleoptera:
932 Curculionidae: Lixinae). *Annales de la Société Entomologique de France* 47: 101-
933 111.
934 Hoebeke ER, Beucke K. 1997. Adventive *Onthophagus* (Coleoptera: Scarabaeidae) in
935 North America: geographic ranges, diagnoses, and new distributional records.
936 *Entomological News* 108: 345–362.

937 Howden F, Cartwright OL. 1963. *Scarab beetles of the genus Onthophagus North of*
938 *Mexico*. Washington: Smithsonian Institution.
939 Hunter JS III, Fincher GT.1996. Distribution of *Onthophagus depressus*: an introduced
940 species of dung beetle. *Journal of Agricultural Entomology* 13: 319-322.
941 Matthews EG. 1966. A taxonomic and zoogeographic survey of the Scarabaeinae of the
942 Antilles. *Memoirs of the American Entomological Society* 21: 1-133.
943 Matthews EG. 1972. A revision of the Scarabaeinae dung beetles of Australia. I. Tribe
944 Onthophagini. *Australian Journal of Zoology* 9 (suppl.):1-330.
945 Moczek AP. 2006. Integrating micro- and macroevolution of development through the
946 study of horned beetles. *Heredity* 97: 168-178.
947 Monaghan MT, Inward DG, Hunt T, Vogler AP. 2007 A molecular phylogenetic
948 analysis of the Scarabaeinae (dung beetles). *Molecular Phylogenetics and*
949 *Evolution* 45: 674-692. doi:10.1016/j.ympev.2007.06.009.
950 Moretto P. 2009. Essai de classification des *Onthophagus* Latreille, 1802 africains des
951 5ème et 6ème groupes de d'Orbigny (Coleoptera, Scarabaeidae). *Nouvelle Revue*
952 *d'Entomologie* 25: 145-178.
953 Olson DM, Dinerstein E, Wikramanayake ED, Burgess ND, Powell GVN, Underwood
954 EC, D'Amico JA, Itoua I, Strand HE, Morrison JC, Loucks CJ, Allnutt TF,
955 Ricketts TH, Kura Y, Lamoreux JF, Wettengel WW, Hedao P, Kassem KR. 2001.
956 Terrestrial Ecoregions of the World: A New Map of Life on Earth. BioScience 51:
957 933-938.
958 Palestrini C. 1992. Sistematica e zoogeografia del genere *Onthophagus*, sottogenere
959 *Proagoderus* Lansberge. *Memorie della Società entomologica italiana* 71: 1-358.
960 Paulian R. 1980. Insects of Saudi Arabia. Coleoptera: Scarabaeoidea (1ère contribution).
961 *Fauna of Saudi Arabia* 2: 141-154.
962 Philips TK. 2011. The evolutionary history and diversification of dung beetles. In:
963 Simmons LW, Ridsdill-Smith TJ eds. *Ecology and evolution of dung beetles*.
964 Blackwell Publishing: Oxford. 21-46.
965 QGIS Development Team (2016). QGIS v2.16. Geographic Information System User
966 Guide. Open Source Geospatial Foundation Project. – Electronic document,
967 Available at: http://download.osgeo.org/qgis/doc/manual/<DOCUMENT>.
968 Rambaut A. 2014. FigTree v1.4.2. Available at: http://tree.bio.ed.ac.uk/software/.

969 Roggero A, Barbero E, Palestrini C. 2015. Phylogenetic and biogeographical review of
970 the Drepanocerina (Coleoptera, Scarabaeidae, Oniticellini). *Arthropod Systematic*
971 *and Phylogeny*, 73: 153-174.
972 Roggero A, Barbero E, Palestrini C. 2016. Revised classification and phylogeny of an
973 Afrotropical species group based on molecular and morphological data, with the
974 description of a new genus (Coleoptera: Scarabaeidae: Onthophagini). *Organisms*
975 *Diversity & Evolution*. DOI: 10.1007/s13127-016-0297-z [online first version,
976 30.7.2016].
977 Rohlf FJ. 2012. NTSYSpc: numerical taxonomy system. ver. 2.21r. Setauket, New
978 York: Exeter Software.
979 Rohlf FJ. 2016a. tpsDig v2.27. Available at: http://life.bio.sunysb.edu/morph/.
980 Rohlf FJ. 2016b. tpsUtil v1.69. Available at: http://life.bio.sunysb.edu/morph/.
981 Rohlf FJ. 2016c. tpsSmall v1.33. Available at: http://life.bio.sunysb.edu/morph/.
982 Rohlf FJ. 2016d. tpsRelw v1.65. Available at: http://life.bio.sunysb.edu/morph/.
983 Schatzmayr A. 1946. Gli scarabaeidi coprofagi della Libia e dell'Egitto. Atti della
984 Società italiana di Scienze Naturali 85: 40-84.
985 Sharkey MJ, Carpenter JM, Vilhelmsen L, Heraty J, Liljeblad J, Dowling APG,
986 Schulmeister S, Murray D, Deans AR, Ronquist F, Krogmann L, Wheeler WC.
987 2012. Phylogenetic relationships among superfamilies of Hymenoptera. *Cladistics*
988 28: 80-112. doi: 10.1111/j.1096-0031.2011.00366.x.
989 Smith UE, Hendricks JR. 2013. Geometric morphometric character suites as
990 phylogenetic data: extracting phylogenetic signal from gastropod shells.
991 *Systematic Biology* 62: 366–385.
992 Sole CL, Scholtz CH. 2010. Did dung beetles arise in Africa? A phylogenetic hypothesis
993 based on five gene regions. *Molecular Phylogenetics and Evolution* 56: 631-641.
994 doi:10.1016/j.ympev.2010.04.023.
995 Staines CL, Whittington AE. 2003. Chrysomelidae (Coleoptera) types in the Royal
996 Museum of Scotland Collection. *Zootaxa* 192: 1-8.
997 Tagliaferri F, Moretto P, Tarasov SI. 2012. Essai sur la systématique et la phylogénie
998 des *Onthophagus* Latreille, 1802, d'Afrique tropicale appartenant au septième
999 groupe de d'Orbigny. Description d'un sous-genre nouveau et de trois espèces
1000 nouvelles (Coleoptera, Scarabaeoidea, Onthophagini). *Catharsius La Revue* 6:1-

31.

Tarasov SI, Solodovnikov AY. 2011. Phylogenetic analyses reveal reliable morphological markers to classify mega-diversity in Onthophagini dung beetles (Coleoptera: Scarabaeidae: Scarabaeinae). *Cladistics* 27: 1-39.

White F, Leonard J. 1991. Phytogeographical links between Africa and Southwest Asia. In: Engel T, Frey W, Kürschner H. eds. *Contributiones Selectae ad Floram et Vegetationem Orientis*. Flora et Vegetatio Mundi. Band IX. Berlin: Cramer, 229-246.

Wirta H, Orsini L, Hanski I. 2008. An old adaptive radiation of forest dung beetles in Madagascar. *Molecular Phylogenetics and Evolution* 47: 1076-1089. doi:10.1016/j.ympev.2008.03.010.

Woodruff RE. 1973. *Arthropods of Florida. Vol 8. The scarab beetles of Florida (Coleoptera: Scarabaeidae)*. Gainesville: Florida Dpt. of Agricolture.

Yu Y, Harris AJ, He X. 2010a. A Rough Guide to S-DIVA v1.9. Available at: http://mnh.scu.edu.cn/S-DIVA/blog/SDIVA/index.html.

Yu Y, Harris AJ, He X. 2010b. S-DIVA (Statistical Dispersal-Vicariance Analysis): A tool for inferring biogeographic histories. *Molecular Phylogenetics and Evolution* 56: 848–850.

FIGURES

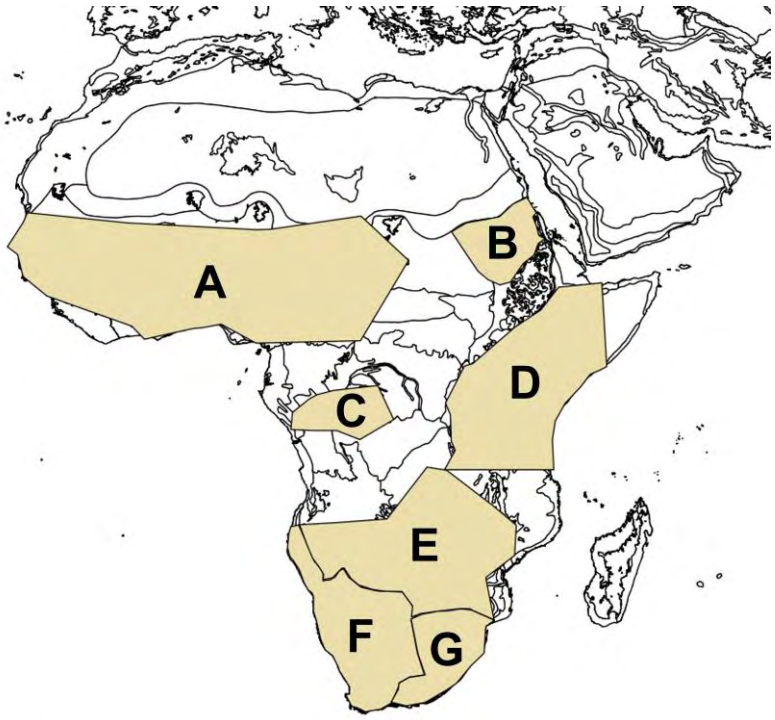

Figure 1. Macroareas identified for the biogeographical analysis, where A = Guinea-Congolian area (GCA), B= Eastern Sudanian area (ESA), C= Central Congolian area (CCA), D = Somalo-Masai area (SMA), E = Zambesian area (ZAA), F = Namib-Kalahari area (NKA), G = Highveld area (HIA), while the outgroup distribution (H = Oriental Region, ORA) is not shown on the map.

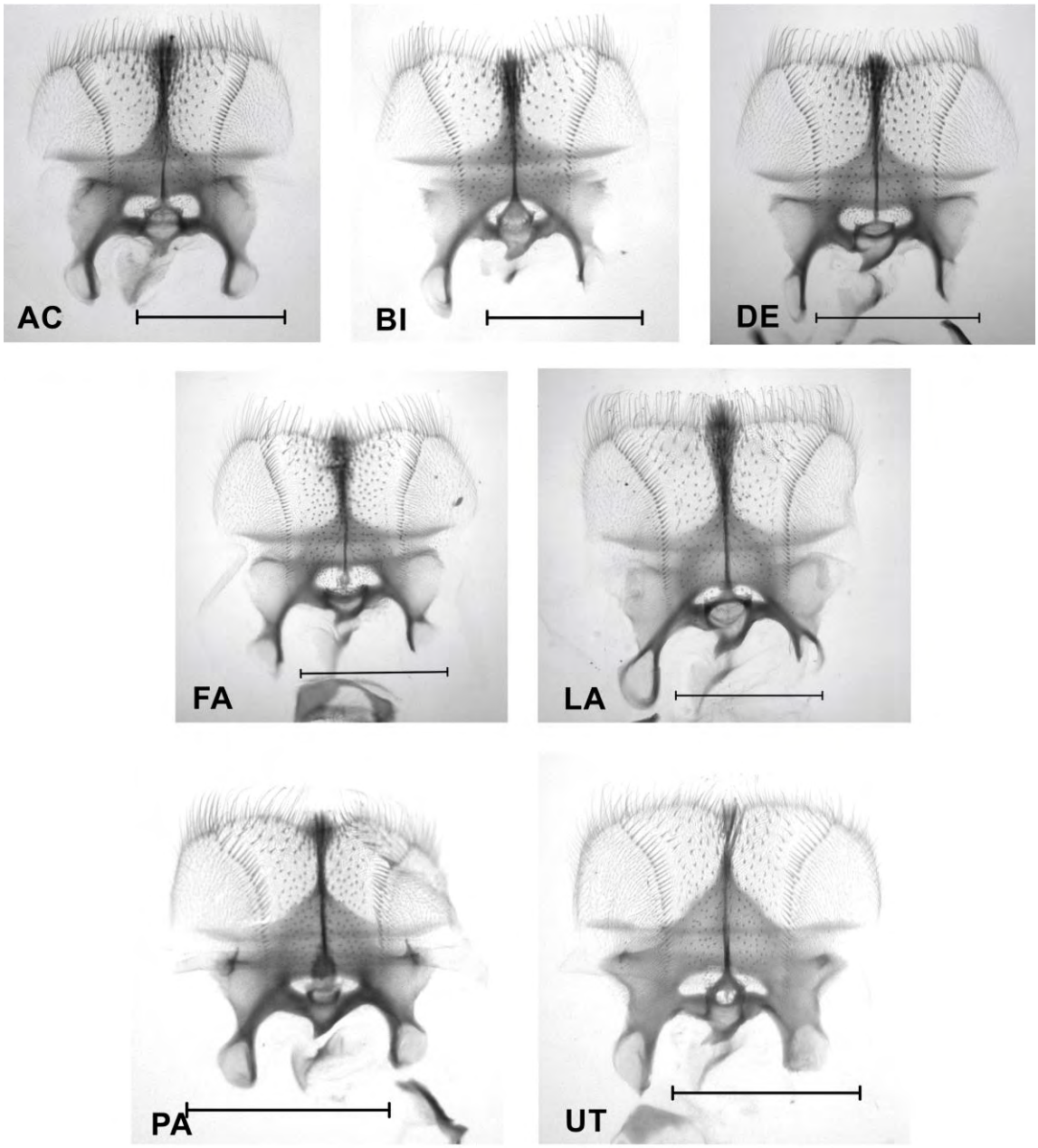

Figure 2. Epipharynx of the species of the genera *Hamonthophagus* (AC = *acutus*, BI = *bitubeculatus*, DE = *depressus*, FA =*fallax*, and LA = l*aceratus*) and *Morettius* (PA = *pallens*, and UT = *utete*). Scalebar = 0.5 mm.

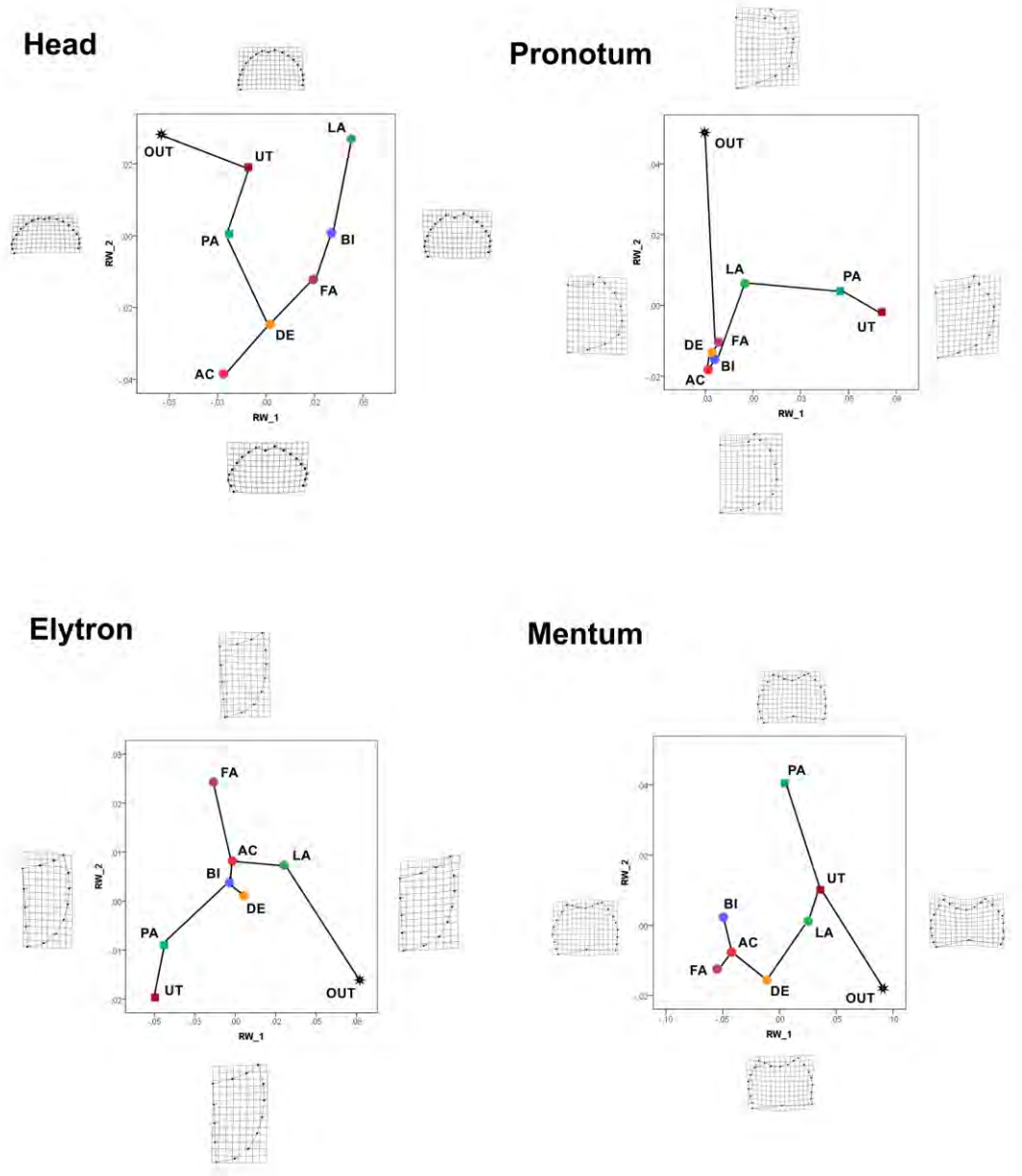

1034

1035 **Figure 3.** Scatterplots of the RW 1 and 2 of head, pronotum, right elytron and mentum
1036 (semilandmarks method). Only the specimens employed to build the matrix are shown
1037 here. The deformation grids corresponding to the minimum and maximum values of the
1038 axes are shown for each anatomical trait. See text for the codes.

1039

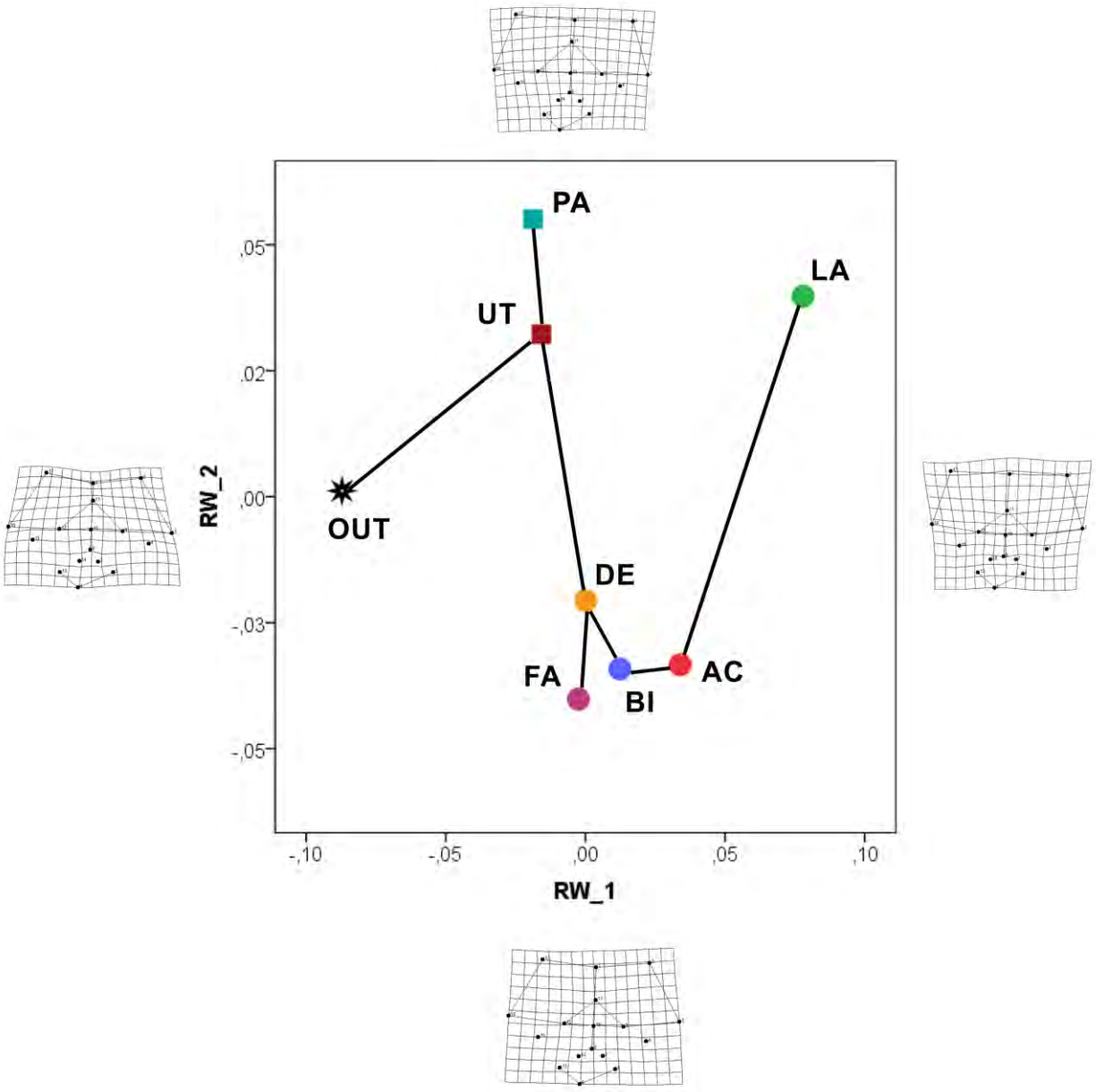

1040

1041 **Figure 4**. Scatterplots of the RW 1 and 2 of epipharynx (landmarks method). Only the
1042 specimens employed to build the matrix are shown. The deformation grids of the
1043 minimum and maximum values of the axes are shown. See text for the codes.

1044

1045

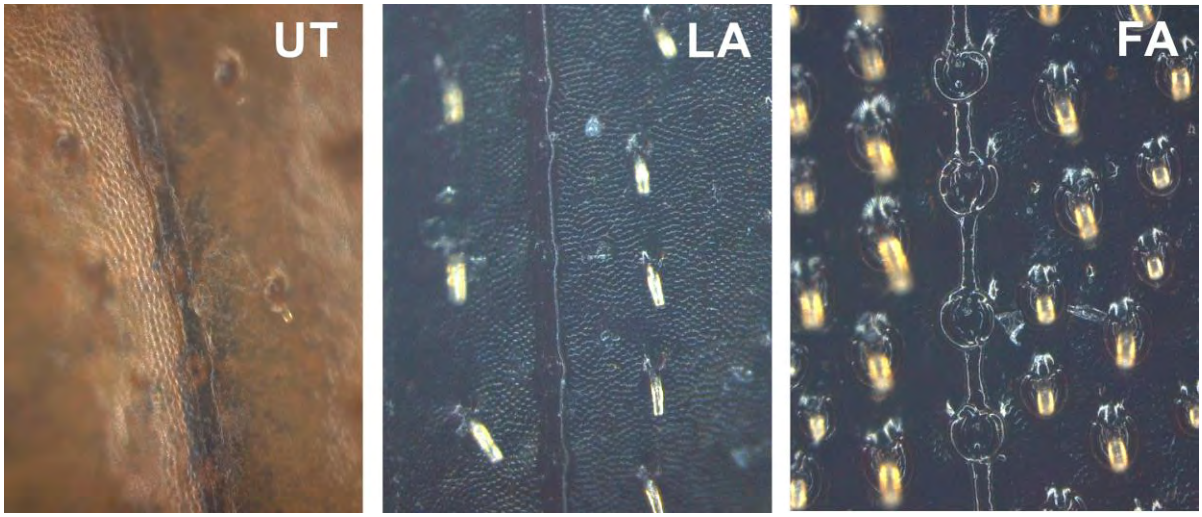

Figure 5. Elytral stria, character 7: from left to right state 0 (*Morettius utete* = UT), state 1 (*Hamonthophagus laceratus* = LA), and state 2 (*H. fallax* = FA).

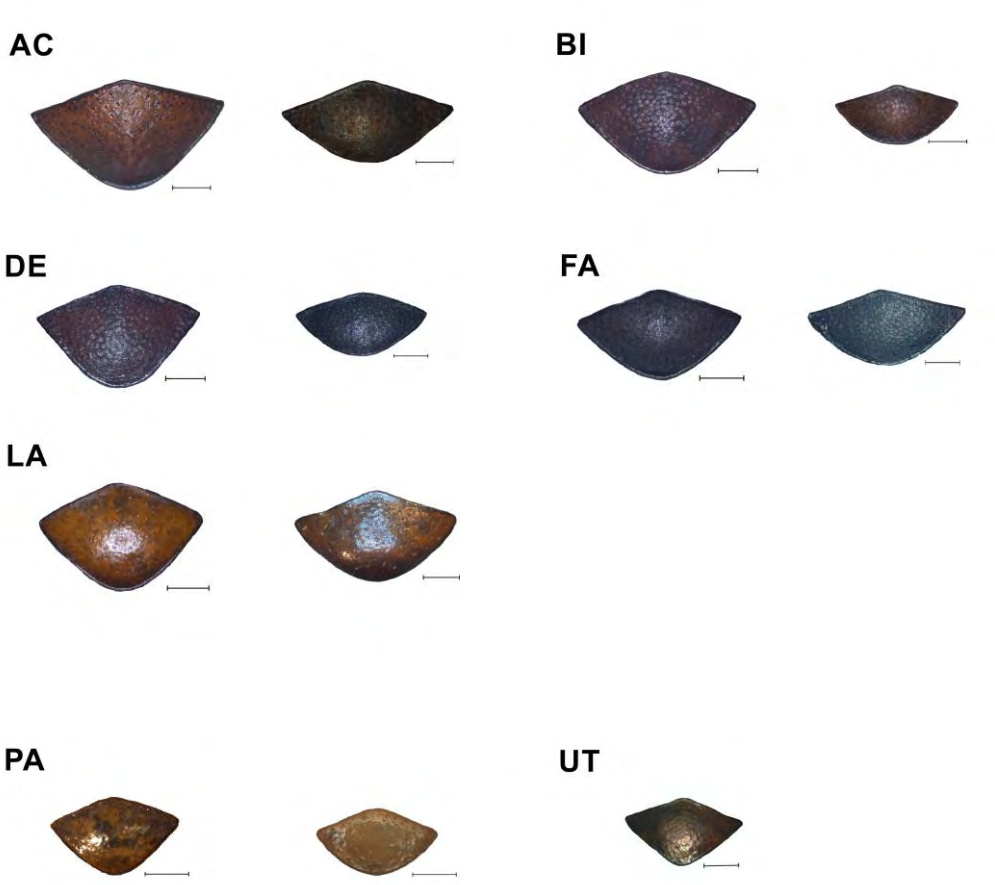

1051

1052 **Figure 6.** Pygidium, male on left and female on right, except *Morettius utete* (UT) in
1053 which only the female is known, see text for the codes. Scalebar = 0.5 mm.

1054

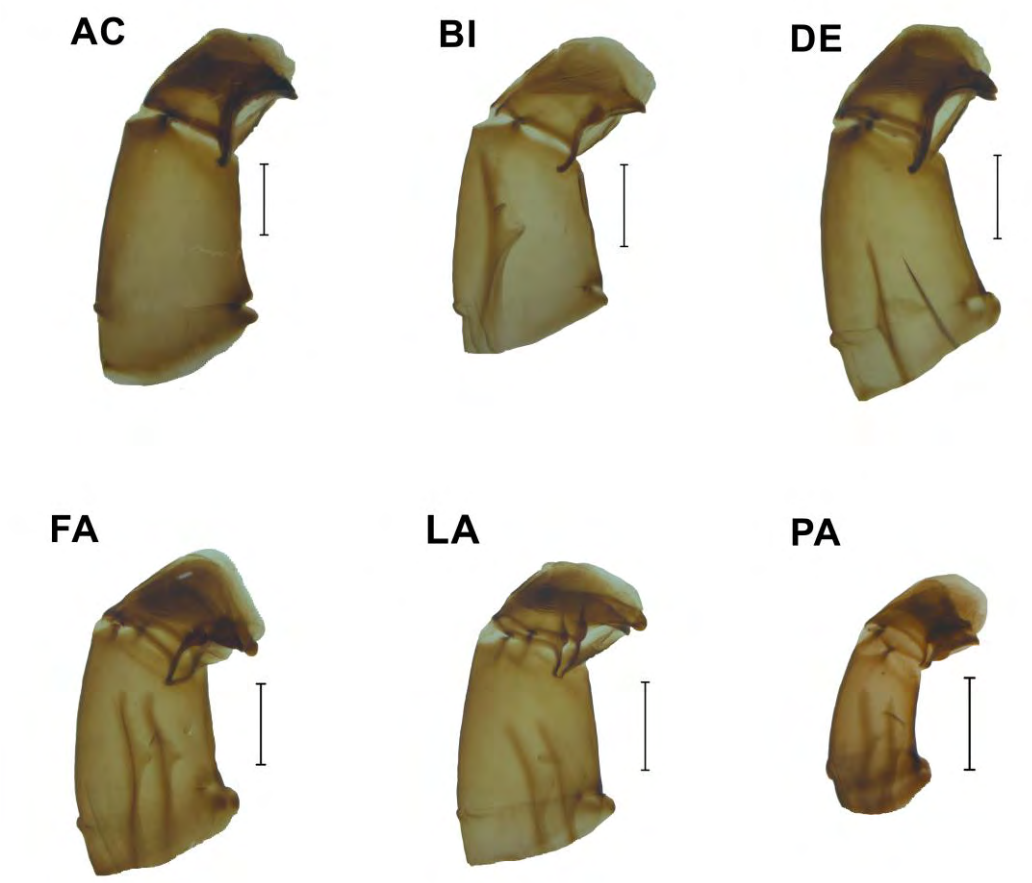

1055

1056 **Figure 7.** Aedeagus of the species of the genera *Hamonthophagus* (AC, BI, DE, FA and
1057 LA) and *Morettius* (PA), see text for the codes. Scalebar = 0.5 mm.

1058

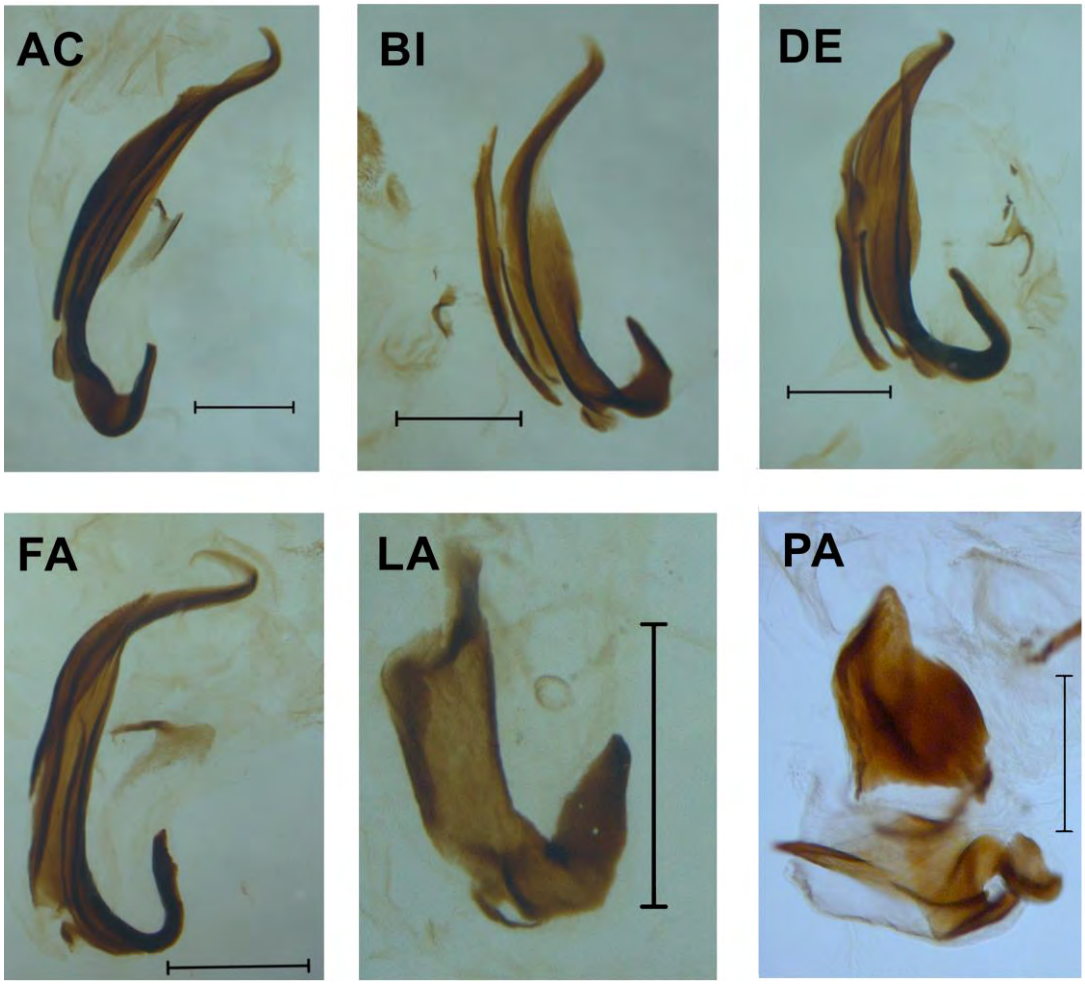

Figure 8. Primary lamella of the species of the genera *Hamonthophagus* (AC, BI, DE, FA and LA) and *Morettius* (PA). Scalebar = 0.5 mm.

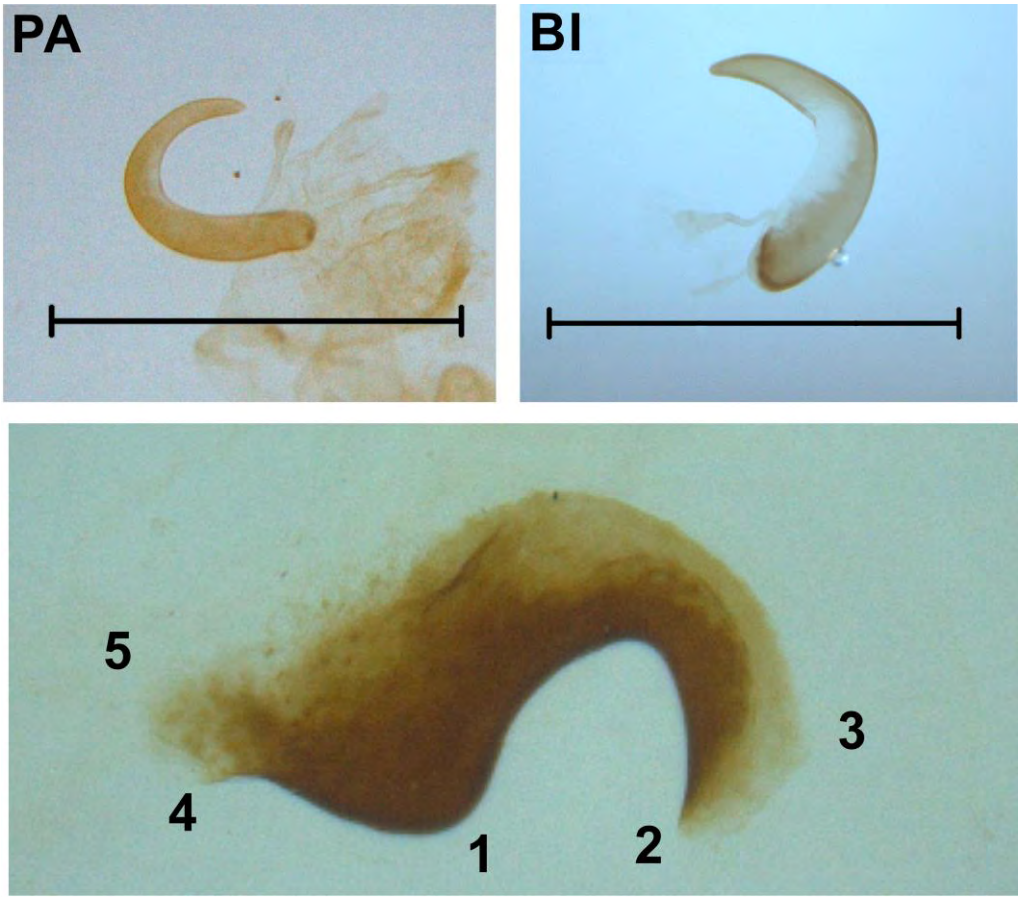

Figure 9. Above, the receptaculum seminis, the features that characterize the two models are clearly represented by *H. bituberculatus* (BI) and *M. pallens* (PA). Scalebar = 0.2 mm. Below, a generic example of the vagina sclerotization (*H. bituberculatus*), after being cleared from membranes and cut off. The various parts were numbered (see text for further details).

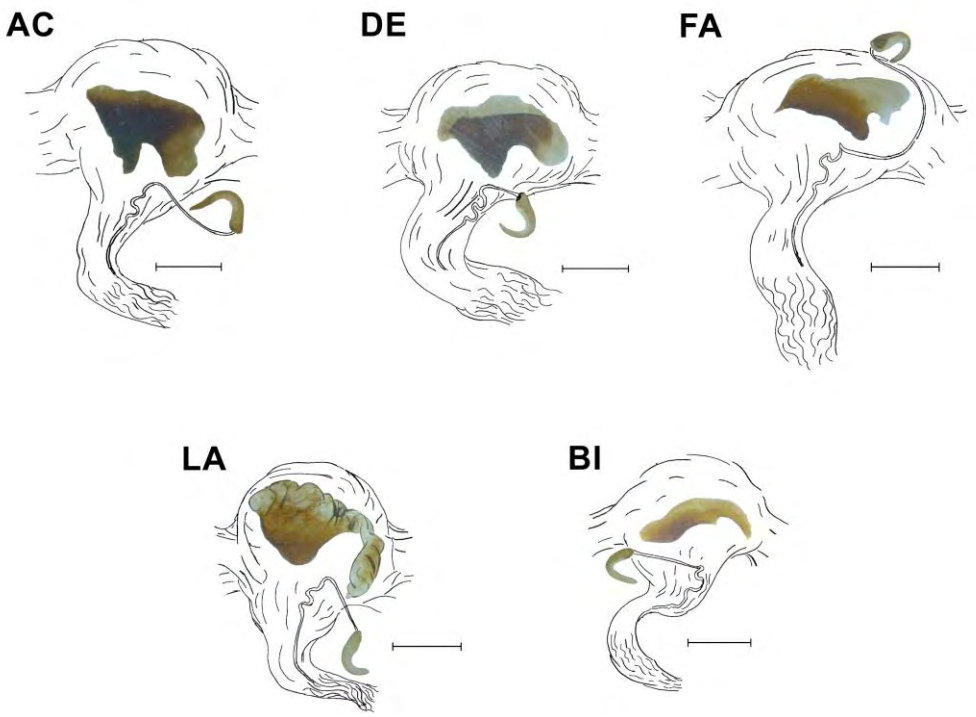

Figure 10. Vagina and receptaculum seminis of the species of the genus *Hamonthophagus* (AC, BI, DE, FA and LA). Scalebar = 0.5 mm.

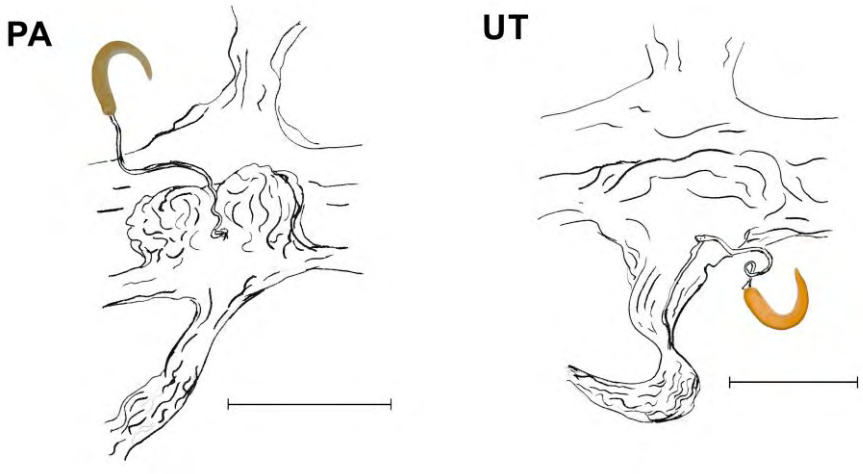

Figure 11. Vagina and receptaculum seminis of the species of the genus *Morettius* (PA and UT). Scalebar = 0.5 mm.

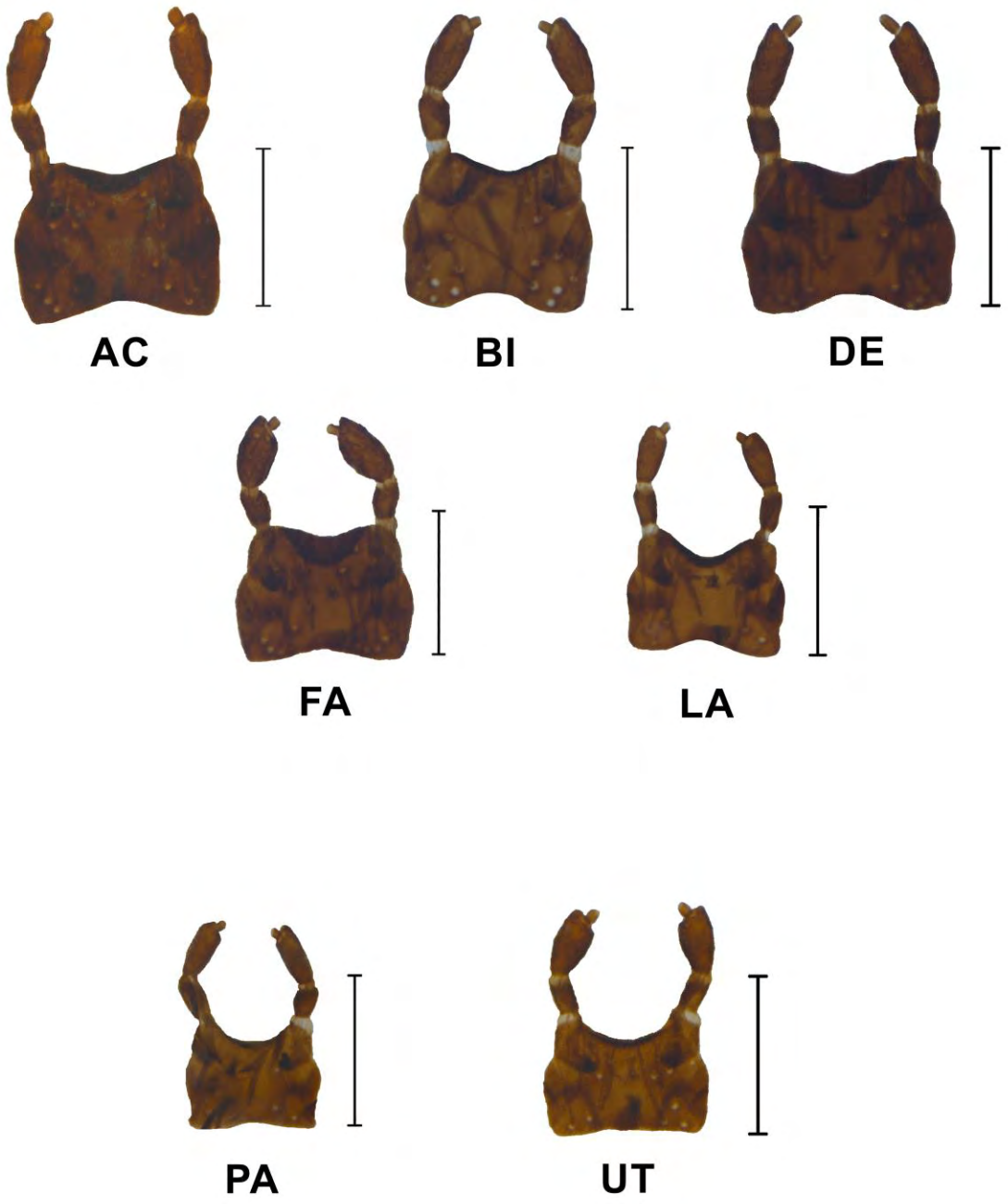

Figure 12. Mentum of the species of the genera *Hamonthophagus* (AC, BI, DE, FA and LA) and *Morettius* (PA and UT). Scalebar = 0.5 mm.

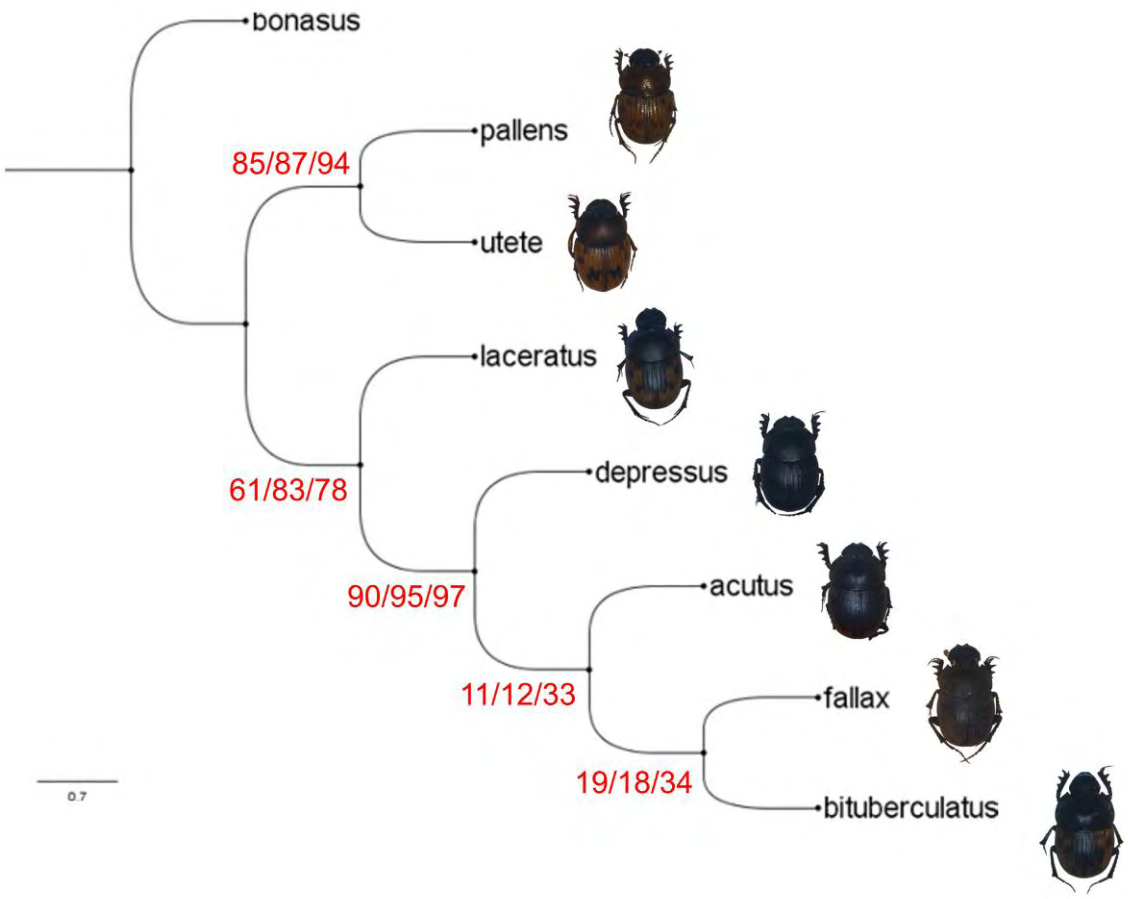

Figure 13. Tree from combined analysis, CI = 0.718 and RI = 0.625. Resampling values are shown on the branches (Standard Bootstrap, Symmetrical Resampling, and Jackknife).

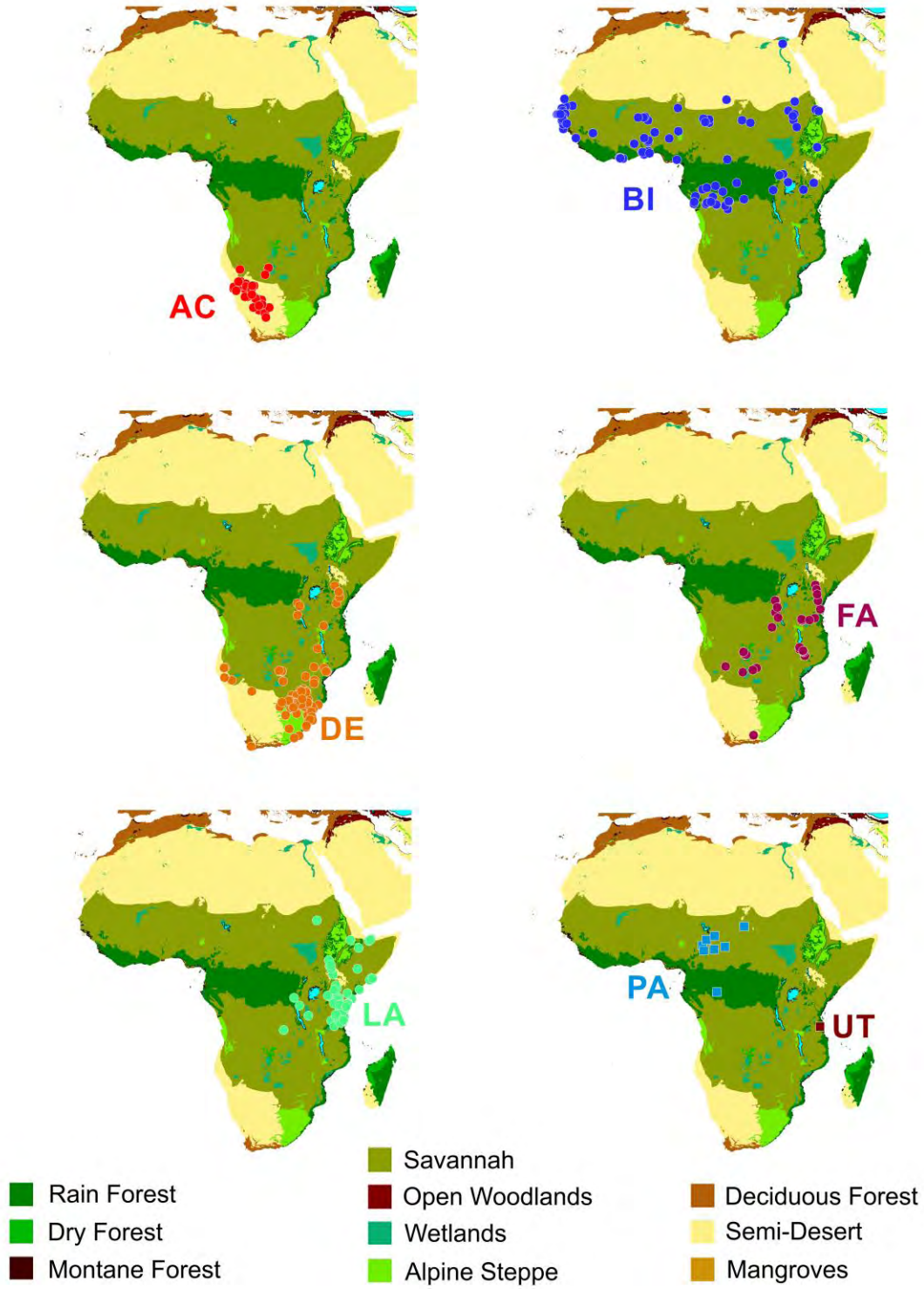

Figure 14. Distribution of the species (see Appendix 2 for the list of the localities) with the Olson et al. (2000) terrestrial biomes classification.

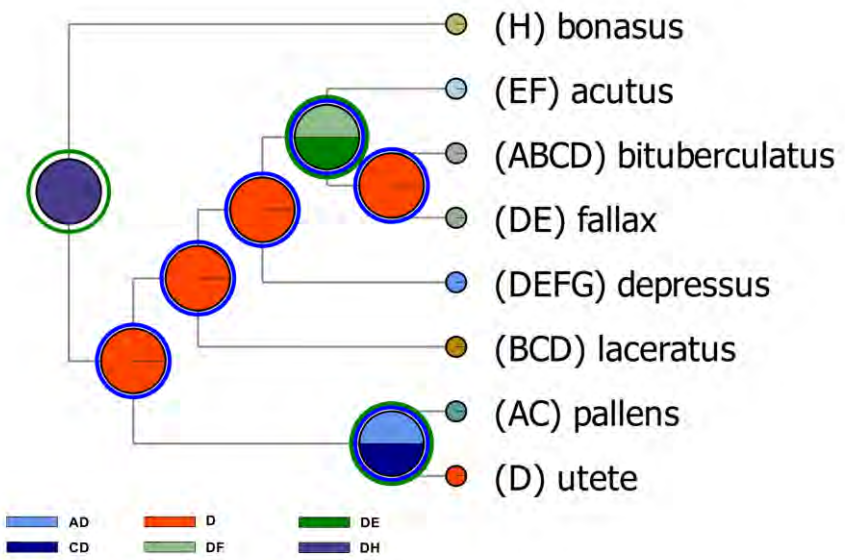

Figure 15. Dispersal-Vicariance analysis, with the legend of the ancestral areas. On the nodes, the dispersal events are marked by a blue ring, and vicariant events by a green ring.

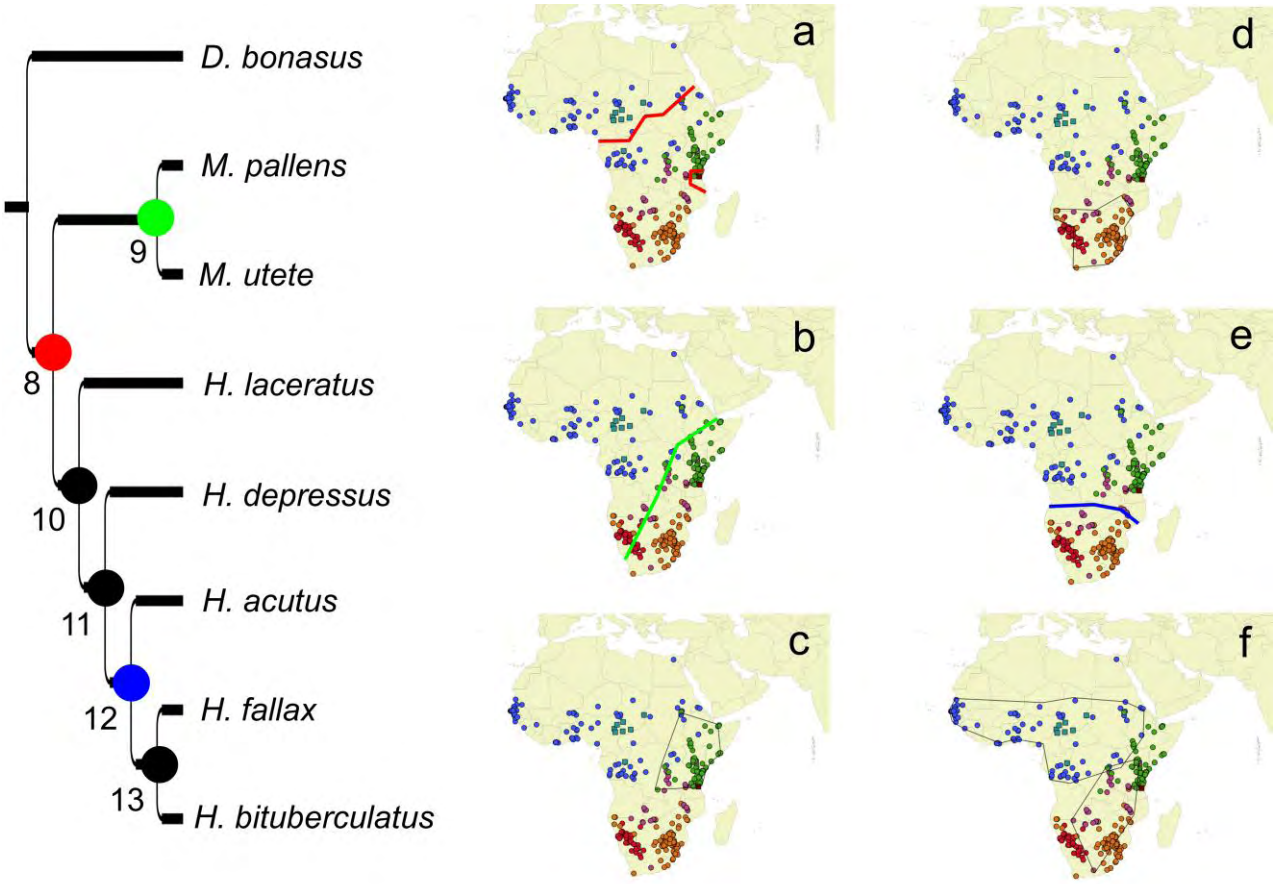

Figure 16. VIP analysis, with the vicariant (red, green and blue dots, respectively) and dispersal (black dots) events marked on the nodes of the tree. Each node is numbered on the tree. The vicariant barriers are shown on the general distribution map (a, b and e), while the species distribution is indicated for dispersal events (c, d and f).

Figure 17. *Morettius utete* **sp. nov.**, paratype female facies. Scalebar = 1 mm.

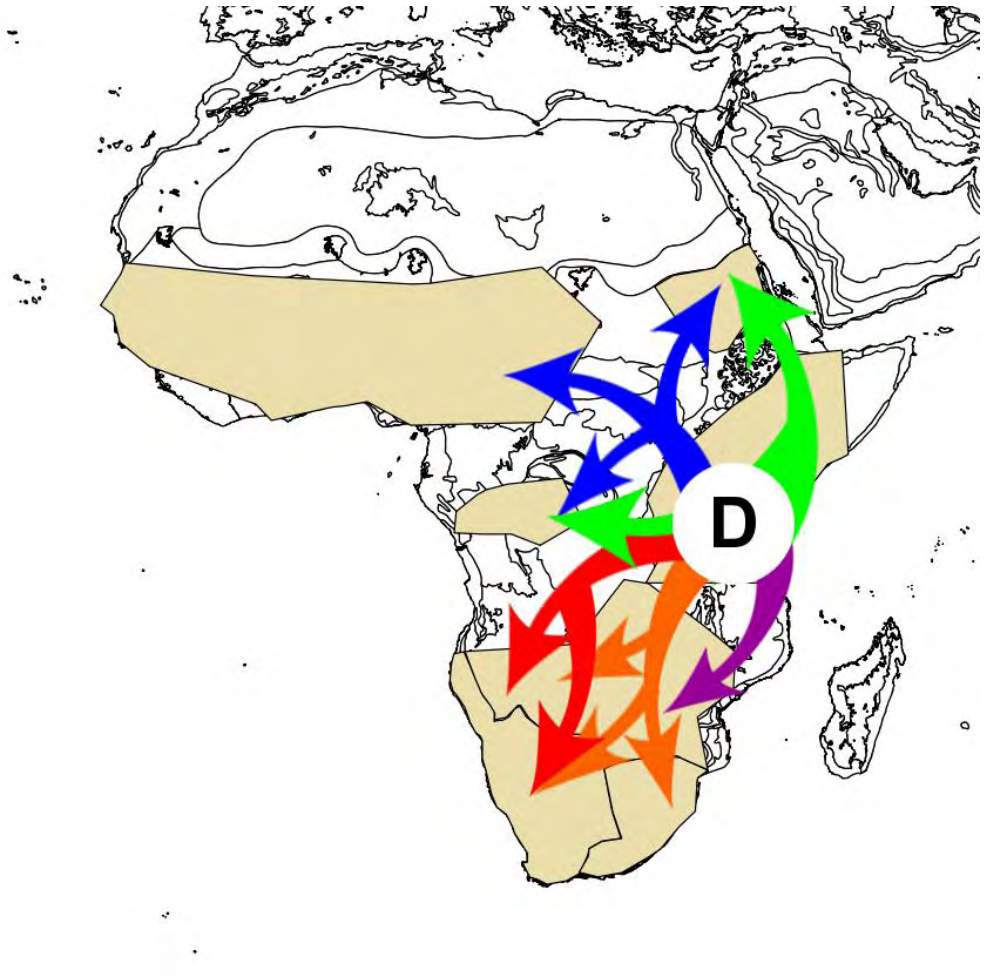

Figure 18. Map showing the *Hamonthophagus* dispersal events that have led to the current distribution. Blue arrow = *H. bituberculatus*, green arrow = *H. laceratus*, red arrow = *H. acutus*, orange arrow = *H. depressus*, and purple arrow = *H. fallax*.